



**University of Thessaly**

**DEPARTMENT OF ELECTRICAL AND  
COMPUTER ENGINEERING**

**Thesis**

*TITLE:*  
**“VLC FOR WIRELESS SENSOR NETWORKS  
APPLICATION DEVELOPMENT”**

«ΑΝΑΠΤΥΞΗ ΕΦΑΡΜΟΓΩΝ ΣΕ ΑΣΥΡΜΑΤΑ ΔΙΚΤΥΑ  
ΑΙΣΘΗΤΗΡΩΝ ΜΕ ΤΗ ΧΡΗΣΗ VLC»

**Vasileios Mousoulis**  
**AEM 513**

**Supervisor professor: Dr. Athanasios Korakis**

**This dissertation is submitted for the degree of Master of Science**  
**Volos, October 2018**

## ABSTRACT

Due to the increase in popularity of using light emitting diode (LED) as the lighting source, it is convenient and easy to provide in-home and in-building visible light communication (VLC) using the already existing LED lamps. The LED-based VLC system offers short-range, license-free and secure communication link. There is no electromagnetic interference (EMI). Several VLC schemes have been proposed and demonstrated.

At the present MSc thesis, the basic concepts describing VLC techniques are presented, included transmitter and receiver modules, modulation methods, and many designing considerations are discussed. Finally a half-duplex VLC system is implemented, giving the opportunity to experiment and study in practice the basic principles of a VLC system.

## ACKNOWLEDGEMENTS

Η παρούσα Διπλωματική εργασία πραγματοποιήθηκε στο τμήμα Ηλεκτρολόγων Μηχανικών και Μηχανικών Υπολογιστών του Πανεπιστημίου Θεσσαλίας, στο πλαίσιο του μεταπτυχιακού προγράμματος «*Επιστήμη και Τεχνολογία Ηλεκτρολόγου Μηχανικού και Μηχανικού Υπολογιστών*», στο Βόλο.

Αρχικά θα ήθελα να ευχαριστήσω τον επιβλέποντα καθηγητή μου, επίκουρο καθηγητή του τμήματος Ηλεκτρολόγων Μηχανικών και Μηχανικών Υπολογιστών, **κ. Αθανάσιο Κοράκη**, που μου έδωσε την ευκαιρία να εμβαθύνω σε ένα τόσο ενδιαφέρον αντικείμενο.

Θα ήθελα επίσης να ευχαριστήσω θερμά τον υποψήφιο Διδάκτορα του τμήματος **κ. Ιωάννη Καζδαρίδη** για την ουσιαστική καθοδήγηση, έμπρακτη βοήθεια και αμέριστη υποστήριξη που μου προσέφερε.

Θα ήταν παράλειψη να μην αναφερθώ στην πολύτιμη συμβολή του καθηγητή κ. Νικόλαου Ανδρίτσου και του ΕΤΕΠ κ. Αναστάσιου Δαφερέρα του Τμήματος Μηχανολόγων Μηχανικών του Πανεπιστημίου Θεσσαλίας, για την θερμή φιλοξενία και υλικότεχνική υποστήριξη που μου παρείχαν στο εργαστήριο «Φυσικών και Χημικών Διεργασιών» του τμήματος.

Τέλος, η μεταπτυχιακές μου σπουδές δε θα ήταν δυνατό να ολοκληρωθούν χωρίς την υποστήριξη της οικογένειάς μου και πιο συγκεκριμένα ευχαριστώ ιδιαίτερα τη σύζυγο μου Ιωάννα για την ενθάρρυνση και την υπομονή της, την Έρη, την Πόπη τη Λιλή και τον Γιώργο που κράτησαν συντροφιά στις μικρές μου κορούλες με πολλή αγάπη όταν και για όσο χρειάστηκε, τον Πρωτεσίλαο για τις συμβουλές του και τις μικρές μου Ευαγγελία και Ερασμία που με την ύπαρξή τους δίνουν μια άλλη διάσταση και νόημα σε όλα.

# CONTENTS

<b>1 VISIBLE LIGHT COMMUNICATIONS .....</b>	<b>10</b>
1.1 GENERAL.....	10
1.2 ADVANTAGES OF VLC .....	11
1.3 APPLICATIONS OF VLC .....	12
1.3.1 Li-Fi .....	13
1.3.2 Vehicle to vehicle communication.....	13
1.3.3 Underwater communication.....	13
1.3.4 Hospitals .....	14
1.3.5 Information displaying signboards .....	14
1.3.6 Visible light ID system .....	15
1.3.7 Wireless local area networks (WLANs) .....	15
<b>2 A VLC SYSTEM.....</b>	<b>17</b>
2.1 BASIC STRUCTURE OF A VLC SYSTEM.....	17
<b>3 LED TYPES.....</b>	<b>19</b>
3.1 LED CIRCUIT MODELS.....	21
3.2 LED DRIVERS FOR COMMUNICATION .....	22
3.2.1 ON/OFF Drivers .....	22
3.2.2 Analog Drivers.....	24
<b>4 PHOTODETECTORS.....</b>	<b>26</b>
4.1 PIN AND AVALANCHE PHOTODIODES .....	27
4.2 LED AS A PHOTODETECTOR.....	28
<b>5 AMPLIFICATION CONSIDERATIONS.....</b>	<b>30</b>
5.1 STABILITY .....	31
<b>6 BASIC MODULATION TECHNIQUES .....</b>	<b>34</b>
6.1 ON OFF KEYING (OOK) – MANCHESTER CODING .....	34
6.2 PULSE MODULATION TECHNIQUES.....	35
6.3 COLOR SHIFT KEYING (CSK).....	36
<b>7 IMPLEMENTATION OF A REAL VLC SYSTEM.....</b>	<b>38</b>
7.1 HARDWARE .....	38
7.1.1 The Transmitter’s hardware .....	38
7.1.2 The Receiver’s hardware .....	42
7.2 SOFTWARE .....	51
7.2.1 Frame format.....	51
7.2.2 Emitter’s code .....	51
7.2.3 Receiver’s code .....	52
7.3 RESULTS.....	55
<b>8 REFERENCES.....</b>	<b>58</b>
<b>APPENDICES .....</b>	<b>60</b>
<b>STANDARDIZATION EFFORTS.....</b>	<b>61</b>

## LIST OF TABLES

TABLE 1. COMPARISON BETWEEN VARIOUS TYPES OF LEDs [21] .....	21
TABLE 2. THE CENTER, CODE AND CHROMATICITY COORDINATES USED BY THE SEVEN BANDS USED IN CSK. ....	36
TABLE 3. DIFFERENT LEDs – DISTANCE PERFORMANCES. ....	38
TABLE 4. TLCR5800 BASIC CHARACTERISTICS. ....	39
TABLE 5. COMPONENT LIST FOR THE DESIGNED VLC RECEIVER. ....	46
TABLE 6. FRAME FORMAT.....	51
TABLE 7. DIFFERENT LEDs -DISTANCE PERFORMANCES USING BOTH THE FINAL DRIVER AND RECEIVER CIRCUITS .....	55
TABLE 8. DISTANCES UNDER DIFFERENT AMBIENT LIGHTING CONDITIONS.....	56

## LIST OF FIGURES

FIGURE 1. FREQUENCY SPECTRUM [3] .....	10
FIGURE 2. VLC FOR VEHICULAR NETWORKS.....	13
FIGURE 3. OPERATION OF UTROV .....	14
FIGURE 4. HOSPI ROBOT [18] .....	14
FIGURE 5. PROTOTYPE PRESENTED BY NEC AND MATSUSHITA ELECTRIC WORKS [71]..	15
FIGURE 6. THE VLC NETWORK SCHEMATIC DIAGRAM [21].....	16
FIGURE 7. GENERAL VLC LINK [51]. .....	17
FIGURE 8. SPECTRAL POWER DISSIPATION AND LUMINOUS MECHANISM OF THE (PC-LED) PACKAGE [54] .....	19
FIGURE 9. DIAGRAM AND SPECTRAL RESPONSE OF A MULTI-CHIP WARM WHITE LED [55]. .....	19
FIGURE 10. MICRO LED [56] .....	20
FIGURE 11. THE SCHEMATIC DIAGRAM OF A TYPICAL RC-LED [57].....	20
FIGURE 12. THE LED'S ELECTRICAL EQUIVALENT CIRCUIT [60] .....	22
FIGURE 13. LED'S DRIVING CURRENT AND ELECTROLUMINESCENCE (EL) WAVEFORM...	22
FIGURE 14. DIGITAL DRIVERS: (A) SINGLE TRANSISTOR, (B) INVERTER, (C) COMPLEMENTARY INVERTER [9] .....	23
FIGURE 15. BAKER CLAMP [9].....	24
FIGURE 16. LED CURRENT DRIVING CIRCUIT: CONCEPTUAL CIRCUIT AND SIGNAL PLUS BIAS COMBINING [61].....	25
FIGURE 17. CARRIER GENERATION DUE TO THE PHOTON ABSORPTION MECHANISM. ....	26
FIGURE 18. PHOTODIODE CURRENT–VOLTAGE CHARACTERISTIC AND MODES [61].....	27
FIGURE 19. (A) PIN AND (B) APD CONSTITUTION AND WORKING PRINCIPLE [61].....	28
FIGURE 20. SPECTRAL RESPONSIVITY OF A LED FUNCTIONING AS DETECTOR AND AS EMITTER [64]. .....	28
FIGURE 21. SPECTRAL RESPONSIVITY OF A LIGHT EMITTING DIODE FUNCTIONING AS DETECTOR, AT DIFFERENT TEMPERATURES [64]. .....	29
FIGURE 22. BASIC OPTICAL RECEIVER AMPLIFYING TOPOLOGIES: (A) OPEN-LOOP CONFIGURATIONS AND (B) FEEDBACK [61].....	30
FIGURE 23. OP AMP BASED, BASIC TIA CIRCUIT [65]. .....	30
FIGURE 24. PHOTODIODE EQUIVALENT CIRCUIT: $I_P$ = PHOTOCURRENT; $R_{SHUNT}$ = DIODE SHUNT JUNCTION RESISTANCE; $C_J$ = JUNCTION CAPACITANCE; AND $R_S$ = SERIES RESISTANCE [65]. .....	31
FIGURE 25. OPEN-LOOP GAIN, $A_{VOL}(j\Omega)$ , AND THE RECIPROCAL OF FEEDBACK FACTOR, $1/B(j\Omega)$ , VERSUS FREQUENCY. THE RATE OF CLOSURE BETWEEN THE TWO CURVES DETERMINES THE LIKELIHOOD OF OSCILLATIONS/RINGING [65]. .....	32
FIGURE 26. PHASE COMPENSATION CAPACITOR $C_F$ HELPS IMPROVE STABILITY [65]. ....	32
FIGURE 27. PHASE RESPONSE WITH THE PHASE-COMPENSATION CAPACITOR, $C_F$ [65].....	33
FIGURE 28. THE OOK MODULATION SCHEME USES MANCHESTER CODING [67] .....	34
FIGURE 29. PULSE MODULATION TECHNIQUES PWM VS PPM [68].....	35
FIGURE 30. VPPM MODULATION TECHNIQUE .....	35
FIGURE 31. CHROMATICITY DIAGRAM [70]. .....	37
FIGURE 32. THE ARDUINO NANO AND TEENSY LC BOARDS .....	38
FIGURE 33. RELATIVE LUMINOUS INTENSITY VS. ANGULAR DISPLACEMENT FOR TLCR5800 .....	39
FIGURE 34. MANCHESTER ENCODED DATA .....	39
FIGURE 35. THE TRANSMITTER CIRCUIT, FIRST ATTEMPT. ....	40
<b>FIGURE 36. THE TRANSMITTER CIRCUIT, 2ND ATTEMPT.</b> .....	41
FIGURE 37. BIT STREAM THAT TURNS ON AND OFF THE TRANSISTOR.....	41

FIGURE 38. SNR VS DISTANCE FOR BOTH TRANSMITTER CIRCUITS.....	42
FIGURE 39. BLOCK DIAGRAM AND DIP 8 PACKAGE OF THE OPT101.....	42
FIGURE 40. SPECTRAL RESPONSIVITY AND SMALL SIGNAL RESPONSE OF OPT101.....	43
FIGURE 41. OPT101 AS A RECEIVER.....	43
FIGURE 42. FLUORESCENT LIGHTS DISTURBANCE.....	44
FIGURE 43. LED AS A RECEIVER V.1.....	44
FIGURE 44. DATA AS RECEIVED FROM TLCD5800 LED (DISTANCE: 10CM) S/N = 26DB	45
FIGURE 45. DATA AS RECEIVED FROM TLCD5800 LED (DISTANCE: 30CM) S/N = 9.5DB	45
FIGURE 46. THE EXPERIMENTAL SETUP.....	46
FIGURE 47. SYSTEM BLOCK DIAGRAM OF THE IMPLEMENTED VLC RECEIVER V.2.....	46
FIGURE 48. LED AS A RECEIVER V.2 – THE VLC RECEIVER AMPLIFICATION CIRCUIT.....	47
FIGURE 49. TIA'S STAGE FREQUENCY RESPONSE.....	47
FIGURE 50. TIA AND OR STAGES SIMULATION OUTPUTS.....	48
FIGURE 51. THE VOLTAGE COMPARATOR STAGE.....	49
FIGURE 52. DATA AT THE RECEIVER'S-V.2 OUTPUT.....	49
FIGURE 53. RECEIVER V.2 PCB – FABRICATION STAGES.....	50
FIGURE 54. RECEIVER V.2 SHIELD.....	50
FIGURE 55. MANCHESTER ENCODING.....	52
FIGURE 56. A FLOW DIAGRAM OF THE EMITTER'S CODE.....	53
FIGURE 57. A FLOW DIAGRAM OF THE RECEIVER'S CODE.....	54
FIGURE 58. LED'S SNR VS DISTANCE.....	55
FIGURE 59. "EYE PATTERN" AT 1KBPS.....	56
FIGURE 60. A SECOND LED EMITTER "IN PARALLEL".....	57

## LIST OF ABBREVIATIONS AND ACRONYMS

- (MFTP) maximum flickering time period
- (ITS) intelligent transport systems
- (VLC) Visible light communications
- (OWC) optical wireless communication
- (IM) intensity modulation scheme
- (DD) direct detection scheme
- (LOS) line-of-sight
- (LDs) laser diodes
- (EL) electroluminescence
- (PIN) P-type, intrinsic, N type
- (APD) avalanche photodiodes
- (TIAs) trans-impedance amplifiers
- (OOK) On – Off Keying
- (PPM) pulse position modulation
- (PSK) phase shift keying
- (Li-Fi) Light Fidelity
- (OR) offset remover
- (VC) voltage comparator



# LIST OF APPENDICES

## *STANDARDIZATION EFFORTS*



## 1.2 Advantages of VLC.

In the nearest decades, wireless connectivity has become one of the basic commodities in our daily life. The rapidly increasing demand for it has resulted in the ubiquitous deployment of wireless systems as well as a heavily congested wireless spectrum that has occurred as a result. In response, VLC has been gaining in popularity as a good complement and substitute for radio frequency due to the following motivations and inherent advantages:

- **Dwindling RF Spectrum [21]:** The RF spectrum is a natural resource of the state, and its usage is regulated to remove signal interference and pollution, as well as for efficient spectral usage [23]. It is cheaper for mobile operators to acquire spectrum, rather than building more base stations to enhance capacity [24]. Furthermore, it reduces the chance for potential future competitors from entering the market. As the demand for wireless data transmission is constantly increasing, the radio frequency spectrum is becoming increasingly congested [25]. Thus the remaining spectrum is dwindling and spectral management is fast becoming a concern [26]. There have been developments to use up the Terahertz frequency range which lies between the RF and microwave spectrum [27], [28], but it would mean creating an entirely new class of infrastructure compatible with the wavelength band. On the other hand visible light has 10,000 times greater spectrum than radio waves (Radio waves correspond to a frequency band of  $\sim 3$  kHz to  $\sim 300$  GHz, while the visible light correspond to a frequency band of  $\sim 400$  THz to  $\sim 780$  THz) [29]. With 12 billion light bulbs in operation around the world with unlicensed, reusable bandwidth, there can be 12 billion potential VLC transmitters.
- **The Capacity Crunch:** Mobile data are expected to have a significant growth the next coming few years. Due to explosions in data usage, there is a major concern for mobile operators to focus on public Wireless Fidelity (Wi-Fi) and other alternative technologies. Level one mobile network operators expect 22% of their capacity they add in 2013 to come from public Wi-Fi and by 2018, 75% of their small cells will have integrated Wi-Fi [31]. These statistics reflect the growth in wireless network usage. The global appetite for wireless broadband data access is increasing by the day, with forecasts of a 18 fold increase in mobile traffic in 2016 compared to 2011, fueled by the smartphone, laptop and tablet popularity. Broadband service providers are introducing usage caps due to high demand and diminishing bandwidth. On the other hand the potential communication bandwidth of visible light ( $\sim 400$  THz) is incomparably wider than the conventional RF bandwidth [32]. As a result in contrast to limited spectra of traditional radio frequency, VLC systems have huge available unregulated bandwidth resource to compliment short-range wireless transmission [33], [34].
- **Interference:** VLC is intrinsically safe and does not cause any interference with RF signals [35]. Thus this technology is perfectly suitable for communication in hospital, industrial and aerospace applications [20].
- **Security:** RF waves pass through walls, and are susceptible to snooping. Since light is confined to an area surrounded by opaque boundaries, there can be well defined coverage zones with enhanced security for VLC.
- **Spatial Reuse:** Since VLC is facilitated by emission of highly directional and confined visible light, there can be coexistence of many non-interfering links in close proximity which allows greater data density [36] and spatial reuse of modulation bandwidth in adjacent communication cells [37], [38].

- **Safety:** In illumination conditions, there are no health hazards of visible light. Unlike IR, visible light satisfies the eye-and-skin safety regulations [38] making it safe for usage in any scenario with far larger emitted optical power [20] giving VLC communication an edge in terms of transmission distance over IR. Furthermore, fluorescent lamps are known to have mercury emissions from broken lamps during their disposal, which can have adverse environmental and health concerns [39], [40]. However, there is recently a lot of attention on the effect of pulsed light on human responses, a study carried out by Katsuura et al. revealed pupillary response under a 100  $\mu$ s pulsed blue light to be significantly higher than under normal conditions [41].
- **Energy Efficiency:** LEDs are energy efficient and highly controllable light sources, allowing them to be part of a Green technology [42]. Thus VLC had emerged as an eco-friendly green communication technology [43], [44]. LEDs roughly use one twentieth the amount of energy of a conventional light source. If all conventional light sources are replaced by LEDs, the global electricity consumption would reduce by as much as 50 percent [42], the CO<sub>2</sub> emissions will reduce by over 10 gigatons and crude oil consumption by 962 million barrels, amounting to financial savings in excess of one trillion dollars, and energy savings of  $1.9 \times 10^{20}$  joules over a decade [45]. According to a recent U.S. Department of Energy report, by the year 2025, SSL technology has the possibility of providing energy savings of up to 217 terawatt-hours (TWh) [46].
- **Moving Towards a Smart Power Grid:** There is inherent benefit to leveraging existing power line infrastructure to provide connectivity while exploiting energy-efficient LED illumination systems for wireless downlink. The ubiquity of LED lighting together with power line networks leads us to conclude that VLC will be a strong complementary wireless technology to indoor PLC much in the way that Wi-Fi currently supports broadband Ethernet connections [20].
- **Easy Implementation into Existing Infrastructure:** VLC can easily be implemented into existing lighting infrastructure with the addition of a few relatively simple and cheap front end components operating in baseband [47]. The VLC transmitters are widely deployed due to their symbiotic relationship with indoor energy efficient lighting [20]. Thus there can be inherent benefits of leveraging on existing lighting infrastructure intended for illumination which has led to significant interest in short range indoor VLC [48].
- **Low Cost:** Another advantage of VLC devices is their comparative low cost. The implementation cost of VLC is less since only a few upgrades of existing lighting infrastructure is required rather than the initial set up cost of an entire communication system. Besides LED infrastructure is also expected to decrease in price and according to the US Department of Energy, by 2017 the dollars per kilo-lumen (\$/klm) pricing of LEDs is expected to decrease roughly by 55% relative to current pricing [50].

### 1.3 Applications of VLC

Inherent features of VLC include high bandwidth, no health hazard, low power consumption and non-licensed channels that made it attractive for practical use. Different application scenarios using VLC are as follows:

### 1.3.1 Li-Fi

In 2011, Harald Haas was the first to coin the term Light Fidelity (Li-Fi) [8,9]. Li-Fi is a high speed bi-directional fully connected, visible light wireless communication system and is analogous to Wi-Fi, which uses radio frequency for communication [10]. The Wi-Fi signals have the problem of interference with other RF signals such as its interference with pilot navigational equipment signals in aircraft [11]. Therefore, in the areas that are sensitive to electromagnetic radiation (such as aircrafts) Li-Fi can be a better solution. A Li-Fi also lends support to the Internet of Things (IoT) [7,12]. A speed up to 10Gbits/s is obtained using Li-Fi, which is 250 times more than the speed of super-fast broadband [13].

### 1.3.2 Vehicle to vehicle communication

VLC can be used for vehicular communication due to the presence of the vehicle lights and the existing traffic light infrastructure. The high priority applications indicated by the Vehicle Safety Communications Project include cooperative forward collision warning, pre-crash sensing, emergency electronic brake lights, lane change warning, stop sign movement assistant, left turn assistant, traffic signal violation warning and curve speed warning [14]. All of the high priority applications require reliable reachability with extremely low latency. Due to the extremely low allowable latency in the vehicle safety communication, a high speed visible light communication system like Li-Fi can be used as shown in Fig. 2. In [15], an outdoor VLC system using Controller Area Network (CAN) was proposed and the back lights and headlights were used in the proposed system for communication.

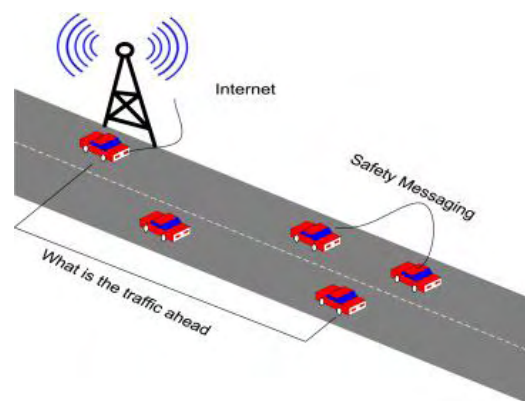


**Figure 2. VLC for vehicular networks**

### 1.3.3 Underwater communication

RF waves do not travel well in sea water because of its good conductivity. Therefore, VLC communication should be used in underwater communication networks [16]. The Un Tethered Remotely Operated Vehicle (UTROV) is another application of the VLC in underwater communication. The different jobs that can be performed using UTROV include observatory maintenance of the oceans and deployment opportunity from the ships. Fig. 3 outlines the operation of the UTROV. The right pane shows the communication of the UTROV using the optical channel to a fixed infrastructure on the sea floor. In the center, the communication is achieved by UTROV

using an optical channel with a ship based relay infrastructure. The left most pane shows the communication of the UTROV using low bandwidth underwater communications.

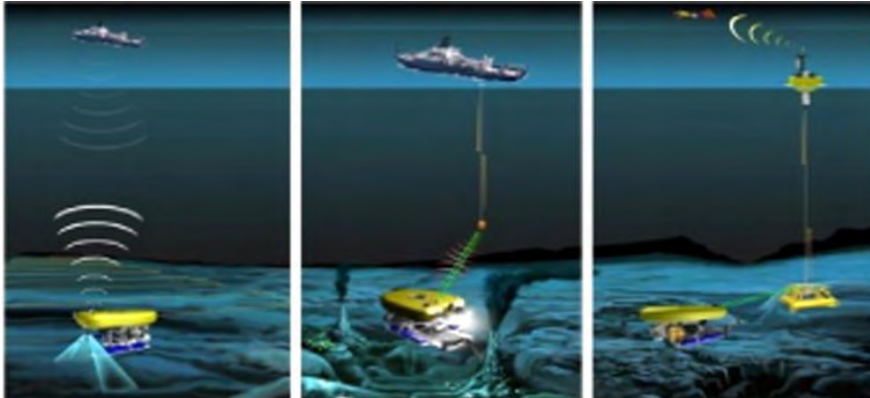


**Figure 3. Operation of UTROV**

### 1.3.4 Hospitals

In hospitals, electromagnetic wave sensitive areas (such as MRI scanners) are likely to switch to VLC because it will not interfere with radio waves of the other machines [17]. In [18], a robot called HOSPI (shown in Fig. 4) was proposed that was used for transportation in hospitals. The control system enhancements in HOSPI were made using VLC installed in a building and navigational sensors of the robot.

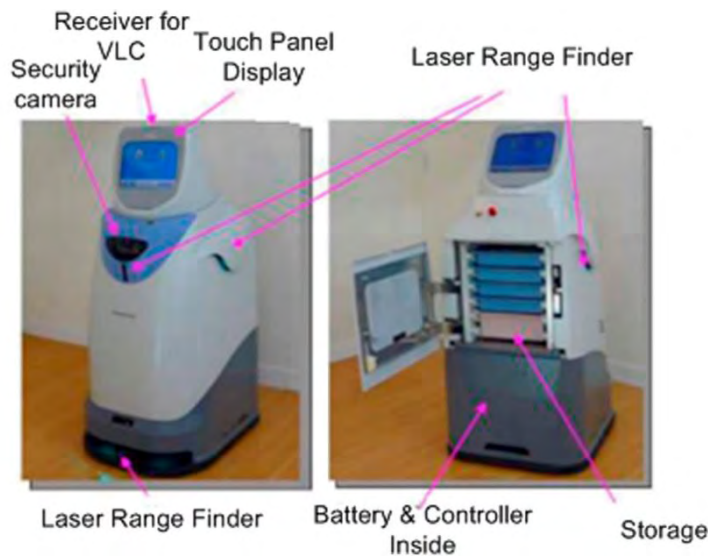


**Figure 4. HOSPI Robot [18]**

### 1.3.5 Information displaying signboards

Signboards are often made from an array of LEDs which in turn are modulated to convey information in airports, bus stops and other places where the broadcasting of data is necessary. In [19], the sign board used for transmitting data was described. This type of sign board can be used for indications in various locations such as airports, museums and hospitals.

### 1.3.6 Visible light ID system

Visible light can be used as an ID system in different places such as buildings and subways. For example, if we are standing in room 12 in a certain building. A visible light ID system can be employed for identifying the room number and its building. Similarly a visible light ID system can be employed in subways, hospitals and airports (figure 5).



**Figure 5. Prototype presented by NEC and Matsushita Electric Works [71].**

### 1.3.7 Wireless local area networks (WLANs)

LED based visible light communication can be used in setting up LANs. In [21], an ultra-high speed full duplex, LAN based on star topology architecture using LED visible light communication is proposed to provide a speed of more than 10-Gb/s and tested for massive users. The schematic diagram of the high speed LAN is shown in Fig. 9[21]. The reason for the design of the network using a star topology is to provide support for massive users. Fiber is used in connection with each lamp directly as shown in Fig. 9. The hybrid access protocol is used in the proposed LAN such as time division multiplexing (TDM) for bidirectional VLC transmission and frequency division multiplexing (FDM) for uplink and downlink fiber transmission. The results of the proposed LAN revealed its potential power of offering high speed access for massive users. In [22], a 10 Mbps VLC wireless LAN system was proposed using white LEDs. The lighting system was used for downlink and infrared light was used for up-link. The VLC wireless LAN has the potential to be used in office buildings and hospitals, which require a high level of safety.

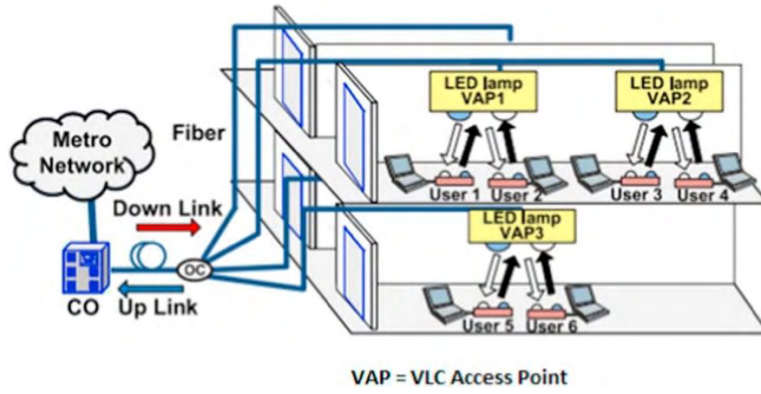


Figure 6. The VLC network schematic diagram [21].



## 2 A VLC SYSTEM

### 2.1 Basic Structure of a VLC System

Since VLC technology provides communication and lighting, typical LED based VLC systems are implemented using an intensity modulation (IM) and direct detection (DD) scheme with a line-of-sight (LOS) configuration due to its illumination purpose [51]. This has several advantages such as the possibility to implement the system using the current state of off-the-shelf illumination components and photo detectors, and a higher bandwidth due to lower path loss and dispersion over short distances [21].

In the transmitter, IM is implemented through the modulation of the transmitted signal into the instantaneous optical power of the LED by controlling the radiant intensity with the forward current through the LED. High modulation frequencies are used to avoid flicker, which can have adverse health effects.

In the receiver, the transmitted signal is recovered using direct detection (DD). In this simple method, a photodiode is used to convert the incident optical signal power into a proportional current. Due to the changes in instantaneous power, DD is the only possible signal recovery process of the signal. Figure 1 shows a general VLC link structure for an IM/DD based VLC system

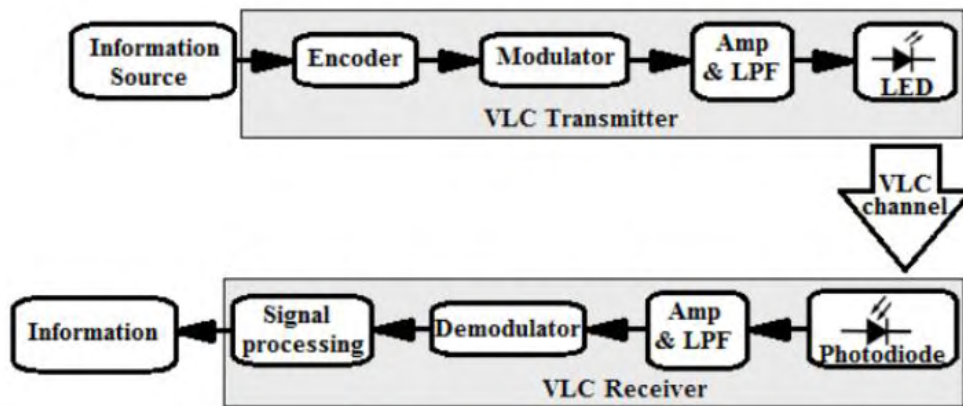


Figure 7. General VLC link [51].

The two main challenges for communication using visible light spectrum are flicker mitigation and dimming support [2].

Flicker refers to the fluctuation of the brightness of light. Any potential flicker resulting from modulating the light sources for communication must be mitigated because flicker can cause noticeable, negative/harmful physiological changes in humans. To avoid flicker, the changes in brightness must fall within the maximum flickering time period (MFTP). The MFTP is defined as the maximum time period over which the light intensity can change without the human eye perceiving it. While there is no widely accepted optimal flicker frequency number, a frequency greater than 200 Hz ( $MFTP < 5$  ms) is generally considered safe [53]. Therefore, the modulation process in VLC must not introduce any noticeable flicker either during the data frame or between data frames.

Dimming support is another important consideration for VLC for power savings and energy efficiency. It is desirable to maintain communication while a user arbitrarily dims the light source. The human eye responds to low light levels by enlarging the pupil, which allows more light to enter the eye. This response results in a difference between perceived and measured levels of light. A lamp that is dimmed to 10 percent of its measured light output is perceived as being dimmed to only 32 percent. Hence, communication support needs to be provided when the light source is dimmed over a large range, typically between 0.1–100 percent.

### 3 LED TYPES

There are different types of LEDs, each with its own special characteristics which make them suitable for different types of applications with specific requirements. Valuable information about different categories of LEDs including key features and a comparison between them can be found in [21]. Here, we summarize some of the most important types of LEDs that can be used for VLC.

- pc-LEDs. The Phosphor Converted LED is a blue LED with a phosphor layer coated on top of it in order to convert part of the blue light to green, yellow and red while the other part of the blue light is leaked out, resulting a mixture which produces white light. These LEDs are low cost but have a bandwidth limitation (the direct modulation frequency is limited to a few MHz) due to the slow response of the phosphor.

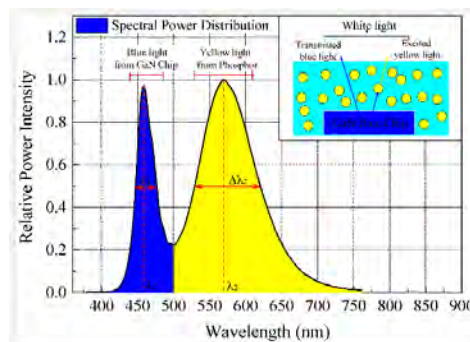


**Figure 8. Spectral Power Dissipation and luminous mechanism of the (pc-LED) package [54]**

- Multi-chip LEDs. These LEDs consist of three or more LED chips which emit different colors, typically Red, Green and Blue (RGB), to produce white light. They have the advantage that colour control can be achieved depending on the light intensities of the different chips, and three individual color channels can be implemented, each providing approximately 15 MHz bandwidth.

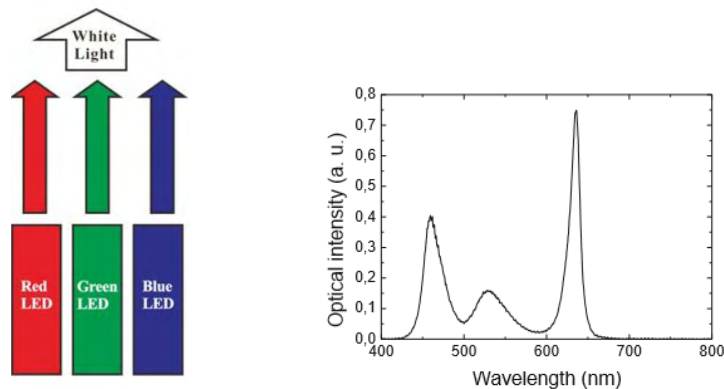


**Figure 9. Diagram and spectral response of a Multi-chip warm white LED [55].**

- Organic Light Emitting Diodes (OLED) OLEDs generate light using an organic layer sandwiched between positive and negative carriers, and are used mainly in flat panel displays. The typical frequency response for OLEDs are in the order of 100's of kHz, far lower than inorganic LEDs which makes OLEDs less suitable for high speed applications. The lifetime of typical white OLEDs is ~50,000 hours, less than the typical inorganic LED lifetime. But since its a more flexible light source than inorganic LEDs, research has been ongoing to improve the frequency response by equalization. Luminous efficacy of 45 lm/W is delivered by OLED panel recently developed by Konica Minolta, however this efficacy was achieved at the cost of a reduced lifetime (LT50 ) of around 8000 hours [21].
- Micro LEDs ( $\mu$ -LEDs). These diode arrays have been in development for VLC recently and have the potential to be used as display panels incorporating high density parallel communication allowing speeds of up to 1.5 Gbps.



Figure 10. Micro LED [56]

- Resonant Cavity LEDs (rc-LED). These LEDs use the resonant cavity method to improve the light extraction efficiency as well as other properties as directionality, intensity and purity. rc-LEDs are particularly suited for optical communication applications, more specifically data communication via Plastic Optical Fiber (POF) and IR wireless communication, but high brightness rc-LEDs would benefit VLC for colour displays. They can be modulated in excess of 100 MHz.

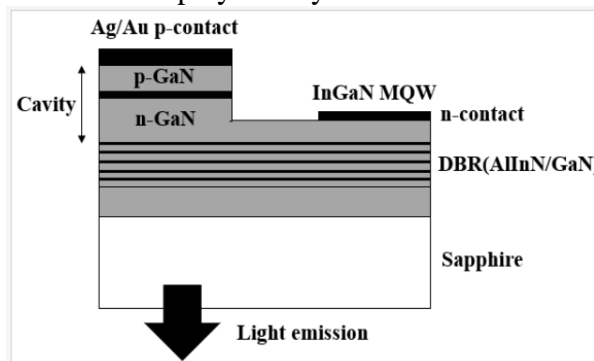


Figure 11. The schematic diagram of a typical rc-LED [57]

- Laser diodes (LDs)[57]. Since it is the photon lifetime, not the carrier lifetime that dominates the dynamics, LDs are capable of handling a data bandwidth enlarged by one or two orders of magnitude greater than LEDs. Thus, in contrast to the limited modulation bandwidth of sub-GHz for LEDs, the modulation bandwidth of LDs is higher than 5 GHz [58]. In addition, LDs has higher current densities and output powers per unit wafer area than LEDs, and recent research has shown that lighting based on multi-colour LDs has no health concern on the human eye. Furthermore, the output light has the feature of coherent and collimated, which is fit for point-to-point data transmission. Thus, by leveraging the advantages

mentioned above, a LD-based white VLC system is promising to outperform the ones based on LEDs. According to the recent studies, multi-Gigabit data rates have been achieved in VLC systems based on III-nitride LDs [59]. However, the safety concerns involving the use of LDs is the main limitation for the rapid development of a LD-based VLC system.

The comparison between these various types of LEDs is presented in Table 1. As it can be seen, each type has its own special characteristics allowing them to be specifically chosen for different types of applications with specific requirements.

Parameter	pc-LED	RGB LED	$\mu$ -LED	OLED
Bandwidth	3-5 MHz	10-20 MHz	$\geq 300$ MHz	$\leq 1$ MHz
Efficacy	130 lm/W	65 lm/W	N/A	45 lm/w
Cost	Low	High	High	Lowest
Complexity	Low	Moderate	Highest	High
Application	Illumination		Bio-sensors	Display

**Table 1. Comparison between various types of LEDs [21]**

### 3.1 LED Circuit Models

The electrical operation of the LED is not much different from a normal P–N junction diode. The current - voltage characteristic of the device has the same form as a normal diode, as given by:

$$I_D = I_o \left( e^{\frac{qV_D}{\eta k_B T}} - 1 \right)$$

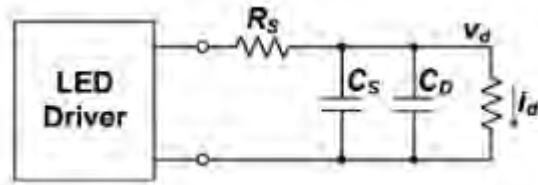
where  $I_o$  represents the device leakage current, when biased in the reverse direction ( $V_D < 0$ ), and  $\eta$  represents a nonideality fitting parameter. As in a normal diode, LEDs also have an intrinsic capacitance  $C_J$ . The intrinsic capacitance of a diode as two major contributing effects:

- (i) the depletion capacitance ( $C_S$ ) due to the presence of a depletion region between P and N sides (this component dominates under reverse biasing conditions) and
- (ii) a second component due to charge diffusion and storage effects under forward bias conditions ( $C_D$ ).

A simple model for the capacitance includes these two contributions:

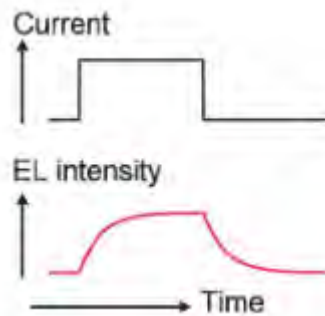
$$C_J = C_S + C_D$$

Figure12 shows the electrical equivalent circuit of the general LED without parasitic elements induced by packaging process. In this figure, the depletion layer capacitance  $C_S$  and the diffusion capacitance  $C_D$  constitute the LED's junction capacitance  $C_J$ .  $R_S$  is the series resistance determined by the LED's structure and resistivity of the p, n regions. A nonlinear resistor represents the I - V characteristic of the LED where  $v_d$  and  $i_d$  are the LED's current and junction voltage, respectively [60].



**Figure 12. The LED's electrical equivalent circuit [60]**

The existence of LED's junction capacitance  $C_j$  as a result, increases rising  $t_r$  and falling time  $t_f$  of the electroluminescence (EL) pulse, especially at high bit-rates (figure 13).



**Figure 13. LED's driving current and electroluminescence (EL) waveform**

## 3.2 LED Drivers for Communication

The design of LED drivers for communications is a challenging task as it entails two distinct areas of electronic design, which often impose conflicting requirements. On one side, the power design advocates the usage of power devices and techniques which most often constrain bandwidth. On the other hand, bandwidth optimization relies on linear behaviour, demanding that the LED remains close to its operating point. However, for power devices this is generally not a reasonable assumption since the device can be subjected to large signal conditions, imposing large changes from its operating point. The design of the LED driver must also take into consideration the type of modulating signals. Two types of drivers can be considered: On/Off drivers—suited for the transmission of digital modulation formats, and analogue drivers—suited for more complex modulation formats demanding continuous or multiple output levels [61].

### 3.2.1 ON/OFF Drivers

Digital LED drivers allow the LED modulation in the digital domain (on–off). The common applications require the LED current control from an input signal that usually has a fixed voltage and low current capability. Thus, an active circuit is needed to drive the required current through the LED. Figure 14 depicts three configurations used in digital LED drivers. The metal-oxide-semiconductor field-effect transistor (MOSFET) is the preferred active device in the digital domain for its low conduction resistance,  $R_{DS\_ON}$ . Thus, at low  $R_{DS\_ON}$  values, the MOSFET can simultaneously handle high currents and achieve low-power dissipation. Nonetheless, bipolar junction transistors (BJTs) can also be used, bearing in mind they require a higher base current to operate (lower input resistance than MOSFETs). Furthermore, they have a lower input maximum voltage specification, which usually requires an additional resistance to limit base voltage

[9]. They also have higher saturation voltage, known as  $V_{CEsat}$ , leading to higher power dissipation when compared to MOSFETs.

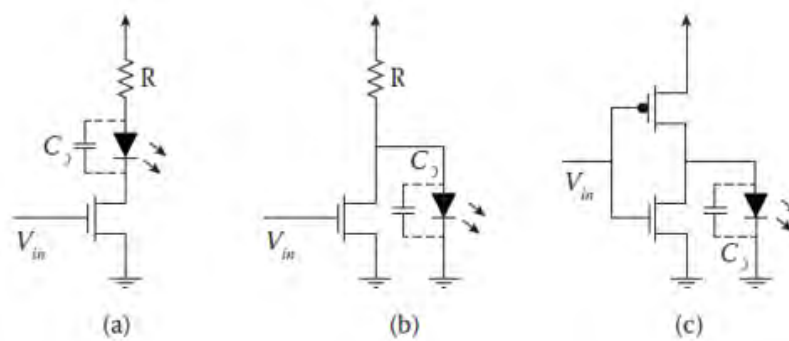


**Figure 14. Digital drivers: (a) single transistor, (b) inverter, (c) complementary inverter [9]**

The circuit in Figure 14a uses a transistor in series with the LED. As  $V_{in}$  increases, the current in the transistor rises, thus the LED current also rises. Considering that the voltage across the transistor is much smaller than the LED forward voltage, the current is limited by the resistor  $R$ , according to Ohm's law, which is given by:

$$I_{LED} = \frac{V_{CC} - V_{LED}}{R}$$

In order to achieve high switching speed, the LED's junction capacitance  $C_J$  must be charged and discharged as fast as possible. As the current rises in the transistor,  $C_J$  begins to charge, limited by the resistor  $R$ . However, when the transistor switches off,  $C_J$  sees a high resistance value and has a slow discharge time [10]. To overcome this issue, it is usually connected a second transistor in parallel with the LED to discharge  $C_J$  when the primary transistor switches off.

However, if a series of several LEDs is used, more than one discharge transistor should be connected to discharge the  $C_J$  effectively in all LEDs. An alternative circuit is shown in Figure 14b. As opposed to the previous example, the LED is active when  $V_{in}$  is in the low state. The on-current is also limited by  $R$  as in (2.48). The disadvantage of this configuration is the asymmetry between  $t_r$  (rise time) and  $t_f$  (fall time) since the LED capacitance is charged through  $R$  and discharged through  $R_{DS\_ON}$ . The third driver circuit uses a complementary metal-oxide semiconductor (CMOS) inverter configuration to drive the LED (Figure 14c). Note that only one transistor is on, except during the on/off transitions. The upper transistor charges  $C_J$  as well as it feeds current to the LED (current source), and lower transistor drains the charge from  $C_J$  (current sink). This circuit allows balancing of the transition times  $t_r$  and  $t_f$  by adjusting transistor parameters [10,11]. In particular, the upper transistor should be dimensioned to be able to drive LED current plus the  $C_J$  charge while the lower transistor must only take care of  $C_J$  discharge. These configurations can drive more than one LED. In order to guarantee the same current for all the LEDs, they are usually arranged in series. However, the transistor must be selected according to the circuit specifications. One of the most important parameters to consider is the maximum allowed voltage across the active device when the control pin is open

( $V_{DSS}$  in MOSFET and  $V_{CEO}$  in BJT). This voltage is commonly known as the breakdown voltage of the transistor. As said, when the device is on, the voltage drop across it is low. However, in the off-state, the device must handle the maximum voltage drop; in other words, the source power voltage value.

### 3.2.1.1 Baker Clamps

BJTs are particularly known by their undesirable saturation region. This region is characterized by having the two junctions forward-biased (base-emitter and base-collector). In this region, the collector current is almost directly proportional to the  $V_{CE}$  voltage. Removing the transistor from saturation is a slow process which can impair the circuit performance.

One technique used to mitigate transistor saturation is the Baker clamp, depicted in Figure 15. It is implemented using a Schottky diode connected between the base and the collector. The principle of a Baker clamp is to reduce transistor gain near the saturation region. In other words, in the active region the diode is in the cut-off state. As the collector voltage decreases near the saturation region, the diode starts to be forward-biased, draining current from the base to the collector. This starts to occur when the collector voltage,  $V_C$ , is approximately 0.3 V (Schottky diode forward voltage) higher than the base voltage,  $V_B$ . Considering a transistor with a  $V_{BE\_ON}$  of 0.6 V,  $V_C$  will be maintained at least 0.9 V higher than the emitter voltage  $V_E$ , thus avoiding transistor saturation. Baker clamps are also used to speed up cut-off time [9]. Assuming the transistor is initially on, when the base current,  $I_B$ , falls to zero rapidly, the collector current  $I_C$  does not decrease as fast as it is desirable. This occurs due to the charges present in the transistor base that need to be drawn. While the base charges are removed, the transistor is in the saturation mode. Using a Baker clamp, the switch-off time is decreased, due to the fact that base charges are drawn through the collector.

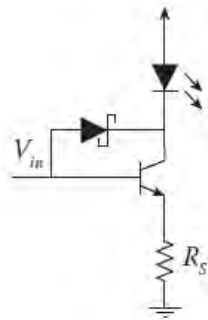


**Figure 15. Baker clamp [9]**

### 3.2.2 Analog Drivers

For more complex modulations such quadrature amplitude modulation (QAM) and orthogonal frequency division multiplexing (OFDM) an analog driver is required [12,13]. Analog drivers should present high linearity. The modulation is assumed for all purposes to be continuous as opposed to the previous case. Two approaches are possible for the design of an analog LED driver: using voltage-mode topologies—where signals are represented by voltages; or using current-mode topologies—where the signals are treated as currents [14]. Regarding circuit theory, current-mode design favors high speed [14]. Using both MOSFETs and BJTs for a given current span, the associated voltage span is a compressed replica. This implies that charging and discharging of the node



parasitic capacitances is faster. On another note, concerning LEDs, current-mode drivers seem more appropriate given the linear power-to-current relationship of the LED.

### 3.2.2.1 Current-Mode Design

Figure 16 depicts a circuit for analog current driving of an LED. This configuration has the LED in series with the transistor and a current sampling resistor  $R_S$ .

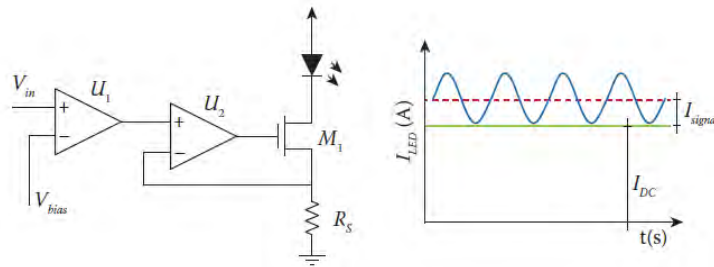


**Figure 16. LED current driving circuit: conceptual circuit and signal plus bias combining [61]**

The transistor input voltage is set by an error amplifier in a feedback loop. By varying its output, the error amplifier will maintain the voltage across  $R_S$  equal to the noninverting input port. The DC bias current is obtained by applying a constant voltage to the input signal,  $V_{bias}$ . One method to define the LED biasing condition is to set the input signal reference voltage at the pre-amplification stage. The operational amplifier  $U_2$  has to be carefully selected. First, it must be able to exhibit large bandwidth. On the other hand, it must be stable under small gain operating conditions (gain close to unity). Although this configuration is more appropriate for LED luminous flux control, the LED bias current flows through the driving transistor (operating in the linear region), thus increasing power dissipation. This problem is also present in  $R_S$ . Furthermore, bearing in mind the driver linearity and intermodulation distortion, the bias current should be selected according to the transistor Characteristics.

## 4 PHOTODETECTORS

In the case of LEDs, the annihilation of an electron–hole pair, more precisely the transition of an electron between conduction and valence bands, was accompanied by the release of energy in the form of a photon of given wavelength. In this case, the process of radiative recombination is explored as a means to generate light of a given wavelength. The opposite process is also possible. In a semiconductor sample exposed to an external light source, the impinging photons arriving at the sample may furnish electrons in the valence band the right amount of energy to move into conduction, through an effect known as photon absorption. These photo-generated electrons are free to move in the semiconductor lattice, and as such, they may serve the purpose of charge carriers under the action of an externally applied electric field (figure 17).

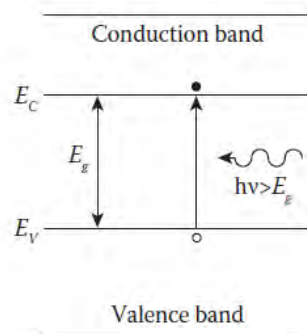


**Figure 17. Carrier generation due to the photon absorption mechanism.**

The photon absorption properties generally depend on the semiconductor material and wavelength.

Figure 18 illustrates the behaviour of the current–voltage characteristic of a typical photodiode. There are three modes of operation that can be employed for optical signal detection:

- the photoconductive mode,
- the photovoltaic mode, and
- the short-circuit mode.

In the photoconductive mode, the photodiode operates under reverse biasing conditions. A typical model for this operation mode represents the photodiode as a current source.

Photodiodes can also be used in direct biasing conditions. This is known as the photovoltaic mode. In this mode, the device output is represented as a voltage, implying a nonlinear logarithmic relation, dependent on the optical radiation exposure. The photovoltaic mode is mainly explored for energy-harvesting applications. For signal detection, the photoconductive mode is more appropriate due to its linearity and sensitivity.

Finally, the short-circuit mode is an intermediate mode where the device feeds a low impedance detector, under absent biasing. This mode is also rarely employed for optical signal detection, due to the fact that the device intrinsic capacitance decreases with the applied reverse biasing. Thus, for large bandwidth applications, the device biasing should be adequately set.

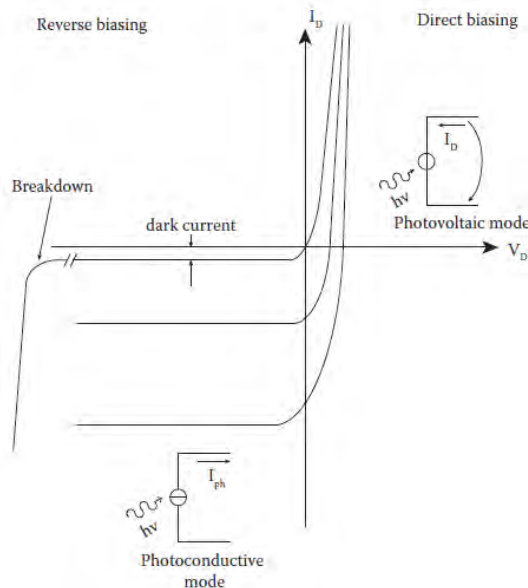


**Figure 18. Photodiode current–voltage characteristic and modes [61].**

## 4.1 PIN and Avalanche Photodiodes

There are two types of photodiodes normally employed for optical signal detection, PIN (P-type, intrinsic, N type) and avalanche photodiodes (APD). PIN photodiodes employ an intrinsic semiconductor layer (sometimes, a lightly doped P-type layer), between the P and N terminals of the device. This layer acts as the optically active region of the device. The device operates in the reverse biasing mode. The photo-generated carriers drift under the action of the reverse electric field through the intrinsic layer and are collected on the P (holes) and N (electrons) sides. The intrinsic layer acts as an extension of the depletion layer of the device. As such it is exploited as a means to augment optical exposure, but also to reduce the device intrinsic capacitance. Figure 19 illustrates the device constitution, its band diagram, and the shape of the electric field.

The APD explores the avalanche effect as a means to improve performance. The avalanche effect occurs under high field regions. Free carriers crossing an intense field region acquire enough energy to generate other free carriers by a process called impact ionization. These generated carriers are on their side accelerated by the electric field and generate more carriers when colliding with the semiconductor lattice. This effect is explored in APD as a current multiplication effect. To achieve this, APDs employ a junction formed by a highly doped N-semiconductor with a P type semiconductor. This junction acts as the current multiplication buffer of the device. The active region, where photon absorption generates the carriers, is formed by an intrinsic layer, terminated with a highly doped P type region. Figure 19 illustrates, for comparison purposes, the APD constitution.

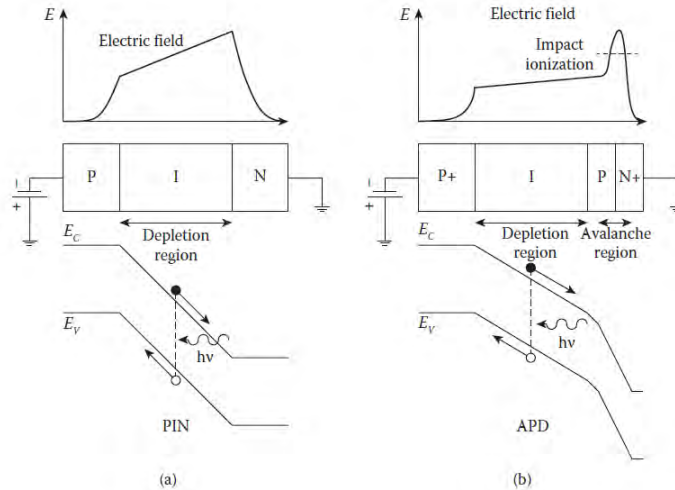


Figure 19. (a) PIN and (b) APD constitution and working principle [61].

## 4.2 LED as a Photodetector

Because LEDs are so commonly used as light emitters it is easy to forget that they are fundamentally photodiodes, and as such, are light detectors as well. Although LEDs are not optimized for light detection, they are very effective at it [62].

A light-emitting diode LED can function as a wavelength selective photodetector whose response is similar to its emission spectral profile. The merit of a LED-based photodetector is its low cost and narrow bandpass response without the need for an additional optical filter [63].

Several restrictions to LED-LED transmission at high data rates apply:

Firstly, not all LEDs have responsivities high enough to provide a power budget sufficient for such a transmission. The longer the emission wavelength of the LED, the higher its responsivity.

It is interesting to note that the responsivity curve is shifted towards lower wavelengths (or higher energy photons) with reference to the peak of LED emission spectra. Obviously, this is because LED cannot detect photons of lower energy than its band gap [63]. As a result the selection of LEDs becomes problematic since there is no a simple relationship between LED emission and detection spectra, see figure 20.

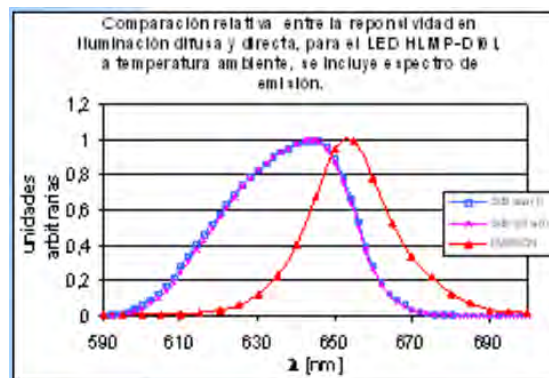
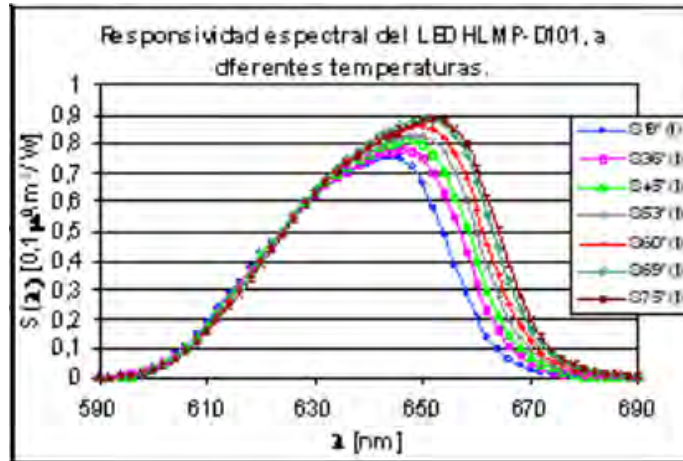


Figure 20. Spectral responsivity of a LED functioning as detector and as emitter [64].

Secondly, a trans-impedance amplifier has to be applied to reduce the time constant formed by the p-n junction, which is high, especially if it is not reversely polarized. In addition,

- the LED band width as detector is wider than its bandwidth as emitter.
- the LED spectral response varies with temperature, see figure 21.
- the LED is highly sensible to changes in the direction of the incident light.



**Figure 21. Spectral responsivity of a light emitting diode functioning as detector, at different temperatures [64].**

## 5 AMPLIFICATION CONSIDERATIONS

The conversion of the PD current into voltage is achieved by front-end circuits designated as trans-impedance amplifiers (TIAs). Trans-impedance amplifiers (TIA's) are used to amplify low-level output current of a photodiode / LED to a voltage level used for high speed data transmission or sensing applications.

TIAs can be divided into two major groups: open-loop and feedback. Figure 22a shows a generic open-loop TIA. Depending on the architecture, open-loop TIAs can be divided into low input impedance amplifiers and high input impedance amplifiers. Low input impedance amplifiers are suitable for high bandwidth and low noise performance applications. However, they present low sensitivity. On the other hand, high input impedance amplifiers have high sensitivity but low-frequency performance. Feedback TIAs (Figure 22b) are usually preferred, mainly because they can overcome the major drawbacks of the others (low sensitivity in low impedance amplifiers, and limited bandwidth in high impedance amplifiers) while keeping their most attractive features (high bandwidth with small input impedance, and high sensitivity with high gains).

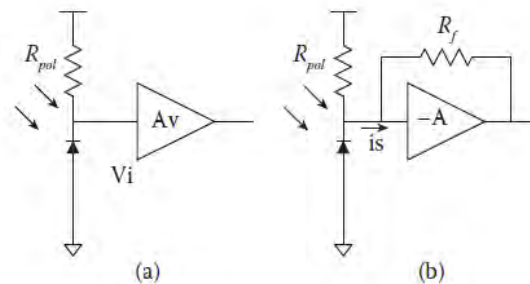


**Figure 22. Basic optical receiver amplifying topologies: (a) open-loop configurations and (b) feedback [61].**

An operational amplifier with a feedback resistor from output to the inverting input is the most straight forward implementation of such a TIA, as shown in figure 23. However, even this simple TIA circuit requires careful trade-offs among noise gain, offset voltage, bandwidth, and stability. Clearly stability in a TIA is essential for good, reliable performance.

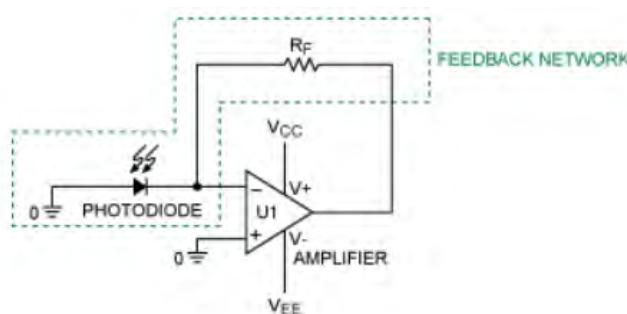


**Figure 23. Op amp based, basic TIA circuit [65].**

## 5.1 Stability

Like any op amp circuit with feedback, each of the above circuits can be separated into an amplifier with open-loop gain,  $A_{VOL}$ , and a feedback network comprised of the resistance and the photodiode. Figure 24 shows the equivalent circuit of the photodiode. For most photodiodes,  $R_{SERIES} = 0$  and  $R_{SHUNT} = \text{Infinity}$  is a fair approximation. Consequently, the simplified model reduces to the short-circuit current source in parallel with the junction capacitance. This simplified photodiode model will be used for subsequent stability analysis.

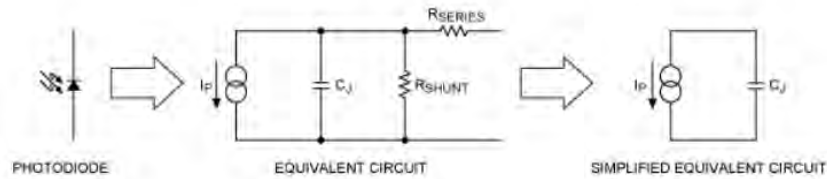


**Figure 24. Photodiode equivalent circuit:  $I_P$  = photocurrent;  $R_{SHUNT}$  = diode shunt junction resistance;  $C_J$  = junction capacitance; and  $R_s$  = series resistance [65].**

To understand why the circuit in Figure23 might oscillate, it is useful to plot the frequency of the open-loop gain and the feedback factor. Figure 25 plots the open-loop gain response of the op amp. It is constant from DC until the dominant-pole corner frequency; it decreases at 20dB per decade thereafter until it reaches the second-pole corner. Mathematically, the single-pole response can be represented as:

Where:

$A_{VOL}$  = DC open-loop gain

$A_{VOL}(j\omega)$  = open-loop gain corresponding to frequency,  $\omega$

$\omega_{PD}$  = dominant-pole frequency in radians/seconds

$$A_{VOL}(j\omega) = \frac{A_{VOL}}{1 + j\left(\frac{\omega}{\omega_{PD}}\right)}$$

Using the simplified equivalent circuit for the photodiode, the feedback network is simply a one-pole RC filter comprised of the feedback resistance,  $R_F$ , and the total input capacitance,  $C_i$  (junction capacitance of the photodiode in parallel with the input capacitance of the op amp). The feedback factor is given as:

$$\beta(j\omega) = \frac{X_{C_i}}{Z_F + X_{C_i}} = \frac{1}{1 + j\omega R_F C_i}$$

Therefore, the reciprocal of the feedback factor is:

$$\frac{1}{\beta(j\omega)} = 1 + j\omega R_F C_i$$

Figure 25 also plots the response curve for  $1/\beta(j\omega)$ . At low frequencies the curve remains flat at unity gain, as expected from the unity-gain resistive feedback. It then rises at 20dB/dec starting from the corner frequency,  $f_F$ .

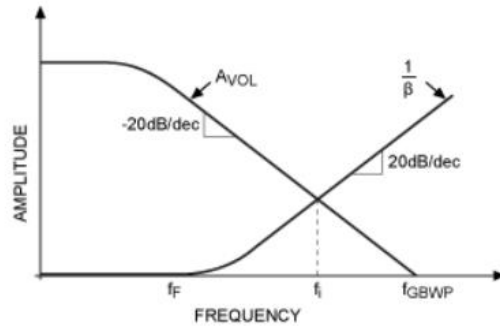


**Figure 25. Open-loop gain,  $A_{VOL}(j\omega)$ , and the reciprocal of feedback factor,  $1/\beta(j\omega)$ , versus frequency. The rate of closure between the two curves determines the likelihood of oscillations/ringing [65].**

From the Barkhausen stability criterion, oscillation can result if the closed-loop TIA circuit does not have sufficient phase margin for  $A\beta \geq 1$ . Hence, the intersection of the  $A_{VOL}(j\omega)$  response curve with the  $1/\beta(j\omega)$  curve denotes a critical intercept fundamental for stability analysis.

It is common knowledge that adding a bypass capacitor in parallel with the feedback resistance provides the requisite compensation to guarantee sufficient phase margin. It is important to calculate the value of the feedback capacitor required to provide optimal compensation.

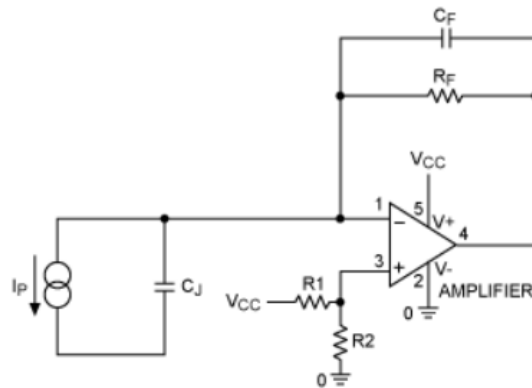


**Figure 26. Phase compensation capacitor  $C_F$  helps improve stability [65].**

To account for the added phase-compensation capacitor, substitute  $Z_F$  in Equation with  $R_F \parallel C_F$ . The feedback factor now becomes:

$$\beta(j\omega) = \frac{X_{Ci}}{R_F \parallel X_{CF} + X_{Ci}} = \frac{1 + j\omega R_F C_F}{1 + j\omega R_F (C_i + C_F)}$$

The addition of capacitor  $C_F$  introduces a zero in the feedback factor, besides modifying its pole. The zero compensates for the phase shift introduced by the feedback network. This can be seen graphically in Figure 27. If the phase shift is overcompensated by choosing a large feedback capacitor, then the rate of closure can be reduced to 20dB per decade (90 degrees phase margin).

However, overcompensation also reduces the usable bandwidth of the TIA. While a reduced bandwidth may not be an issue with low-frequency photodiode applications,



high-frequency or low-duty-cycle pulsed photodiode circuits definitely need to maximize the available bandwidth.

For such applications, the goal is to find the minimum value of the feedback compensation capacitor,  $C_F$ , needed to eliminate oscillation and minimize ringing. However, it is always a good idea to overcompensate the TIA circuit slightly. Overcompensation is recommended to provide sufficient guard band to account for up to  $\pm 40\%$  variation in an op amp's bandwidth over process corners and the tolerance of the feedback capacitor.

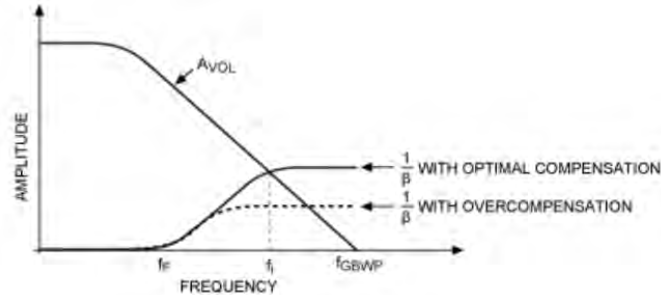


**Figure 27. Phase response with the phase-compensation capacitor,  $C_F$  [65].**

A good design compromise is to target 45 degrees of phase margin at the intercept of the  $A_{VOL}(j\omega)$  and  $1/\beta(j\omega)$  curves. This margin requires the optimum value of  $C_F$  to be calculated so that the added zero in the feedback factor,  $\beta(j\omega)$ , is located at the frequency corresponding to  $A\beta = 1$ , as shown in Figure 27.

It is calculated that the optimal value of the feedback capacitor  $C_F$  is [65]:

$$C_F = \frac{1}{4\pi R_F f_{GBWP}} \left( 1 + \sqrt{1 + 8\pi R_F C_i f_{GBWP}} \right)$$

# 6 BASIC MODULATION TECHNIQUES

Modulation is one of the key processes in communication system. Appropriate and robust modulation techniques allow enhanced performance of the system. The performance of VLC systems is likely to be impaired by the significant high path loss and the shot noise induced by natural and artificial lights. High path loss leads to the use of considerably high optical power levels. In addition, they are also suffered from the speed of optoelectronic devices (LEDs and PIN photodiodes). System performance varies depending on the environment conditions, data rate, technical solutions and implementation of a particular system.

The choice of modulation technique in the design of VLC system remains one of the most important technical issues. Background from IR technology suggests the use of modulation techniques such as OOK, pulse position modulation (PPM) or Pulse Width Modulation (PWM) and these have been discussed and proposed [66].

## 6.1 On Off Keying (OOK) – Manchester Coding

On Off Keying (OOK) is the simplest form of amplitude shift keying (ASK) modulation that represents digital data as the presence or absence of a carrier wave. In its simplest form, the presence of a carrier for a specific duration represents a binary one, while its absence for the same duration represents a binary zero. Some more sophisticated schemes vary these durations to convey additional information [66].

In OOK modulation the LEDs are turned off and on according to the bits in the stream. For example, a “1” is represented by the on state and “0” is represented by the off state. The main advantage of using OOK is its easy implementation

In OOK modulation, the state of LED will greatly depend on the transmitted data. As a result, if we have a lot of “0” data, the LED will be in off state for a long time. It could cause flickering effect of the lighting system in the room.

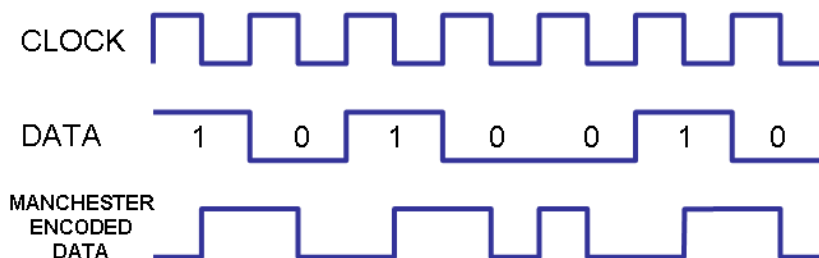


**Figure 28. The OOK modulation scheme uses Manchester Coding [67]**

The 802.15.7 standard uses Manchester Coding to ensure the period of positive pulses is the same as the negative ones but this also doubles the bandwidth required for OOK transmission. Alternatively, for higher bit rates run length limited (RLL) coding is

used which is more spectrally efficient. Dimming is not easily supported in OOK modulation.

## 6.2 Pulse modulation techniques

The limitation of OOK is the low data rates, which motivated researchers to develop new modulation techniques with higher data rates.

**Pulse Width Modulation, (PWM)** varies the width of the pulses according to dimming levels. Using the high PWM frequency, the different dimming levels can be achieved between 0% and 100%

**Pulse position modulation (PPM)** encodes the data using the position of the pulse within a set time period. The duration of the period containing the pulse must be long enough to allow different positions to be identified, e.g. a '0' is represented by a positive pulse at the beginning of the period followed by a negative pulse, and a '1' is represented by a negative pulse at the beginning of the period followed by a positive pulse.

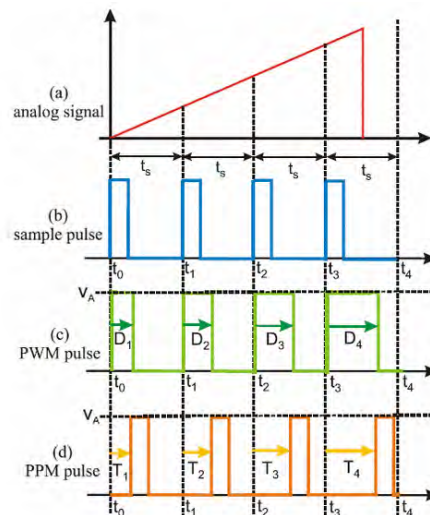


Figure 29. Pulse modulation techniques PWM vs PPM [68]

**Variable pulse position modulation (VPPM)** is similar to PPM but it allows the pulse width to be controlled for light dimming support, as shown in figure 30.

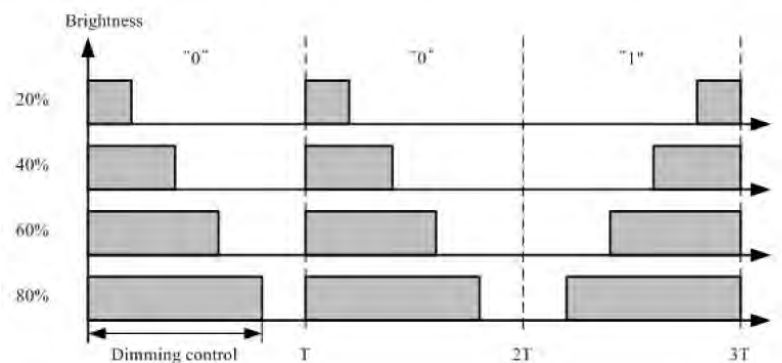


Figure 30. VPPM modulation technique

VPPM modulation technique under dimming helps to achieve variable range and constant data rate. This is achieved by adjusting pulse width. The advantage of this modulation type is that it protects from intra frame flicker. This is due to the fact that pulse amplitude is held constant and dimming is controlled by variable is pulse width.

➔ Here logic '0' is mapped using positive pulse at the beginning of period followed with negative pulse.

➔ Logic '1' is mapped using negative pulse at the beginning of period followed with positive pulse.

For VPPM modulation to be efficient, the duration of period which contains pulses should be long enough so that pulse positions can be distinguished.

### 6.3 Color Shift Keying (CSK)

CSK was proposed in IEEE 802.15.7 to enhance the data rate which was low in other modulation schemes [2]. The switching ability slows down by producing white light utilizing yellow phosphor and blue LEDs. Therefore, an alternate way to produce the white light is the utilization of three separate LEDs such Green, Blue and Red.

Modulation in CSK is performed using the intensity of the three colors in an RGB LED source. CSK depends on the color space chromaticity diagram. It maps all colors perceivable by eye to two chromaticity parameters such as  $x$  and  $y$ . Table 2, illustrates the human visible wavelength seven bands with their centers marked in Fig. 31.

Band (nm)	Code	Center (nm)	( $x$ , $y$ )
380–478	000	429	(0.169, 0.007)
478–540	001	509	(0.011, 0.733)
540–588	010	564	(0.402, 0.597)
588–633	011	611	(0.669, 0.331)
633–679	100	656	(0.729, 0.271)
679–726	101	703	(0.734, 0.265)
726–780	110	753	(0.734, 0.265)

**Table 2. The center, code and chromaticity coordinates used by the seven bands used in CSK.**

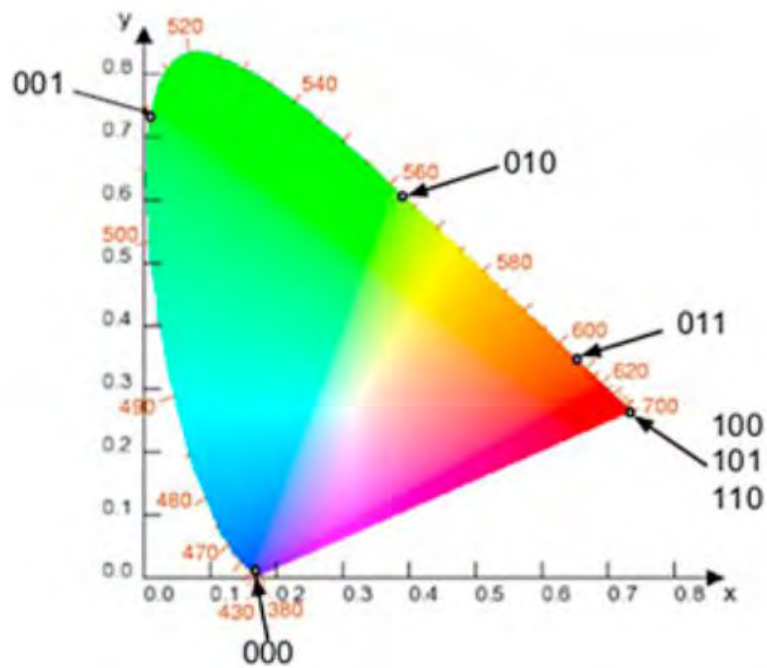


Figure 31. Chromaticity diagram [70].

# 7 IMPLEMENTATION OF A REAL VLC SYSTEM

As part of the current MSc thesis, an Implementation of a real VLC system took place. Many of the topics discussed at the chapters above, were investigated and implemented. The main considerations of designing a real VLC system, is describing in the following chapters.

## 7.1 Hardware

The VLC system design, was based on a microcontroller unit. The idea was to implement and study a low cost, half duplex system, based on a common microcontroller board. Both Arduino nano and Teensy LC boards were selected as appropriate for such an application, since they both are small, inexpensive, complete, and easy to program breadboard-friendly microcontroller boards.

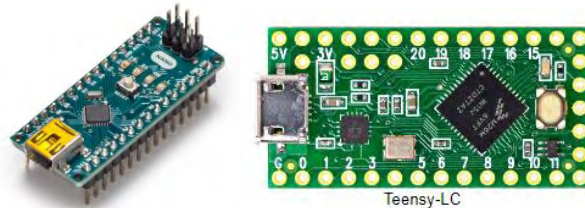


**Figure 32. The Arduino Nano and Teensy LC boards**

### 7.1.1 The Transmitter's hardware

The main considerations when developing the Transmitter module was:

- The proper selection of the LED.
- Selection of the Modulation scheme.
- LED driver's circuit.

#### 7.1.1.1 LED Selection

Many different types of LEDs was investigated: Blue clear, Green, Red ultra – bright, RGB, and pc-white. The same type of LED was used as emitter and receiver. Red clear bright LED found to have the best performance, as shown in table 3.

LED type	Max Distance (1st Driver circuit)	Max Distance (2nd Driver circuit)
Blue clear	7cm	10cm
Red clear ultra-bright	20cm	30cm
Green clear	5cm	8cm
Pc white	10cm	22cm
TLCR5800	48cm	220cm

**Table 3. Different LEDs – Distance Performances.**

After many experimentations and research, TLCR5800, a RED Ultra- bright LED by Vishay was selected.

The TLCx58xx series is a clear, non-diffused, 5 mm power LED for high-end applications where supreme luminous intensity required. This LED with clear untinted plastic case utilize the highly developed ultra-bright AlInGaP (AS). The lens and the viewing angle is optimized to achieve best performance of light output and visibility.

PARTS TABLE														
PART	COLOR	LUMINOUS INTENSITY (mcd)			at I <sub>F</sub> (mA)	WAVELENGTH (nm)			at I <sub>F</sub> (mA)	FORWARD VOLTAGE (V)			at I <sub>F</sub> (mA)	TECHNOLOGY
		MIN.	TYP.	MAX.		MIN.	TYP.	MAX.		MIN.	TYP.	MAX.		
TLCR5800	Red	7500	35 000	-	50	611	616	622	50	-	2.1	2.7	50	AlInGaP on GaAs

Table 4. TLCR5800 basic characteristics.

Its main features include:

- High luminous intensity (typ 35000mcd)
- Angle of half intensity: ± 4°
- Untinted non-diffused lens
- Utilizing ultrabright AlInGaP (AS)
- High operating temperature: T<sub>j</sub> (chip junction temperature) up to 125 °C

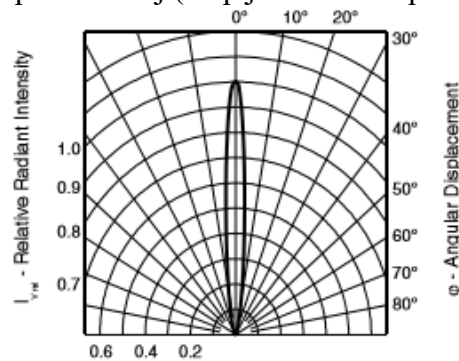


Figure 33. Relative Luminous Intensity vs. Angular Displacement for TLCR5800

### 7.1.1.2 Modulation scheme

As previously mentioned, the simplest modulation scheme for a VLC design, is OOK. Since no special need for high bit rates are required, OOK modulation was selected and implemented.

In OOK modulation, the state of LED depends on the transmitted data. As a result, if a lot of “0” data have to be transmitted, the LED will be in off state for a long time. This could cause flickering effect of the lighting system in the room.

According to the 802.15.7 standard, Manchester Coding is proposed in combination with OOK, to ensure the period of positive pulses is the same as the negative ones.

In the current MSc thesis, OOK modulation with Manchester encoding is selected.

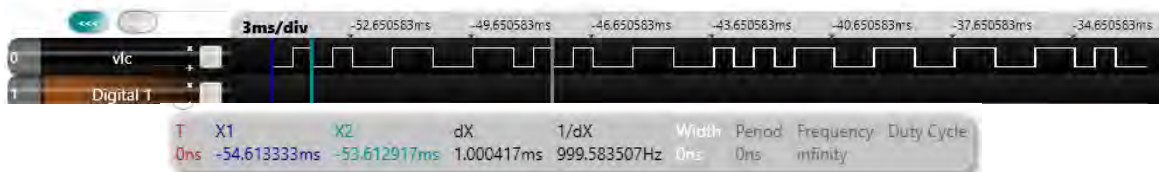


Figure 34. Manchester encoded data

The data is sent with a symbol rate of 1000baud which correspond to a bit rate of 500 bit/s. Depending on the led quality and ambient light, the baud-rate could be increased.

At the bit – rate of 500bit/s, (frequency = 1 kHz), fluctuation of the brightness of light is not noticeable. Flickering time period = 1msec, which is lower than 5msec, the maximum flickering time period (MFTP).

### 7.1.1.3 LED driver circuit

The first approach was to direct drive the LED through the microcontroller's pin. Since the Arduino-nano can provide 5V / 40mA in digital pins, Digital pin D2 was used to drive the emitter's LED.

The result was sufficient concerning throughput at low distances, for such a low cost circuit. Maximum distance of 48cm was achieved with TLCR5800 RED Ultra- bright LED as an emitter (figure35).

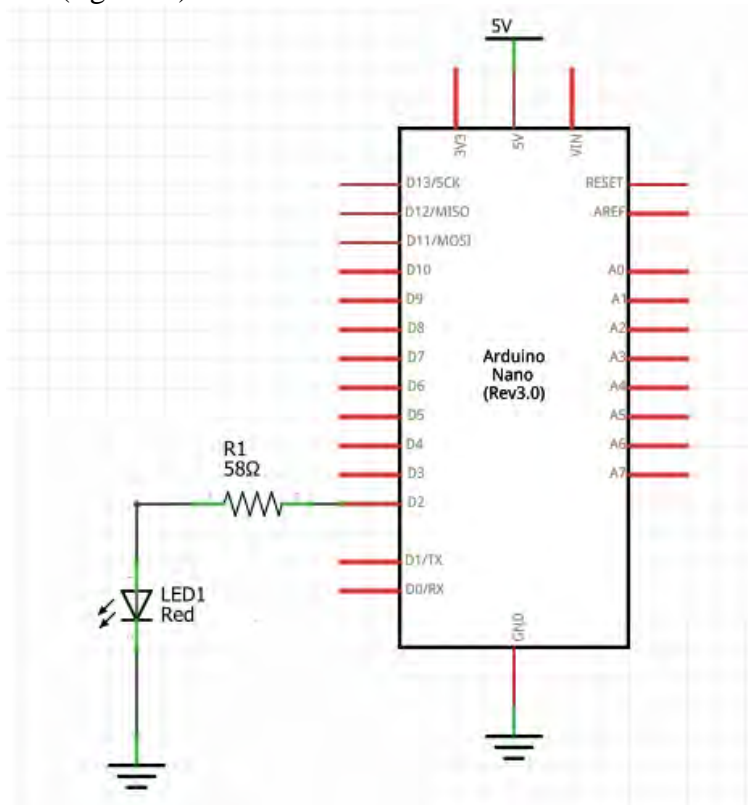


**Figure 35. The transmitter circuit, first attempt.**

A second driver circuit was designed to enhance speed and distance issues. A Digital LED driver, which allows the LED modulation in the digital domain (on–off) was designed. As a semiconductor, the BC546 NPN BJT Transistor was selected (figure 36).



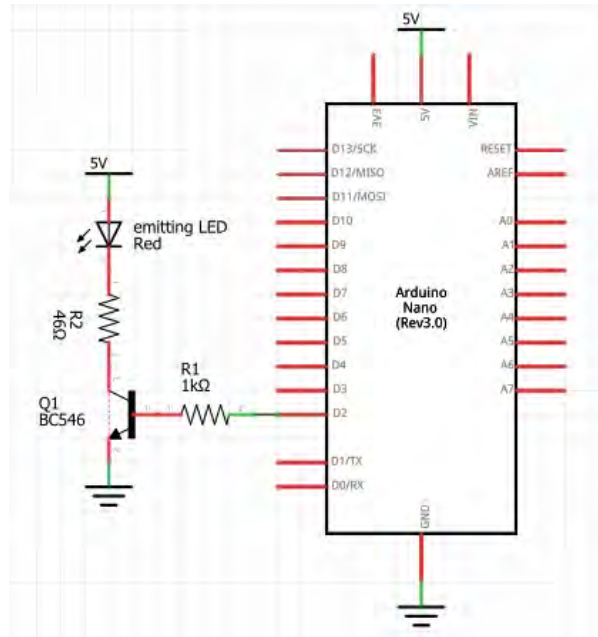


**Figure 36. The transmitter circuit, 2nd attempt.**

The second emitter circuit optimises system’s performance, since it drives the emitting LED with the suggested by the manufacturer continuous forward current ( $I_f$ ) and so the maximum emission power of the LED is achieved. An SNR vs Distance comparison for both transmitter circuits is shown in figure 38.

As TLCR5800 LED requires  $I_f = 50\text{mA}$  at  $2.1\text{V}$ , the values of  $R_2$  resistor is calculated:

$$R_2 = \frac{5V - V_{Led} - V_{ce(sat)}}{50\text{mA}}$$

$$R_2 = \frac{5V - 2.1V - 0.6V}{50\text{mA}}$$

$$R_2 = 46\Omega$$

The bit stream that turns ON and OFF the transistor, as it measured across  $R_2$ , is shown above (figure 37).

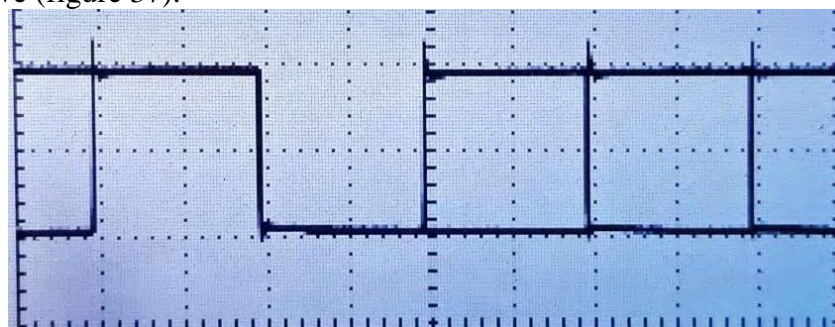


**Figure 37. Bit stream that turns ON and OFF the transistor.**

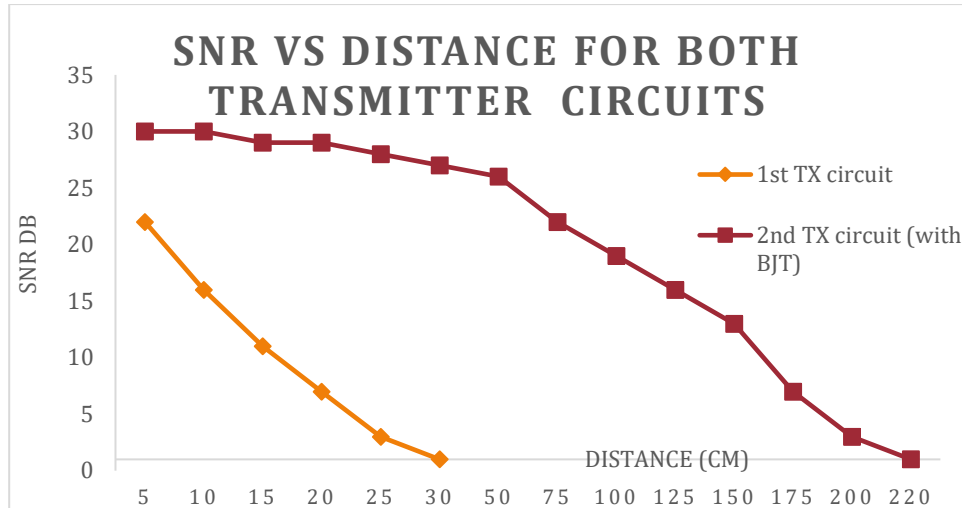


**Figure 38. SNR vs Distance for both transmitter circuits**

### 7.1.2 The Receiver’s hardware

The main hardware considerations when developing the Receiver module include:

- The proper selection of the reception device (photodiode, Led, photovoltaic etc.).
- The Amplification circuit.
- Sufficient Immunisation to Noise / ambient light.

#### 7.1.2.1 OPT101 photodiode as a receiver.

Many experiments and measurements took place in order the optimal reception device to be selected.

In the first attempt, a photodiode was selected. In particular, OPT101 Monolithic Photodiode and Single-Supply Trans-impedance Amplifier by Texas Instruments was tested (figure 41).

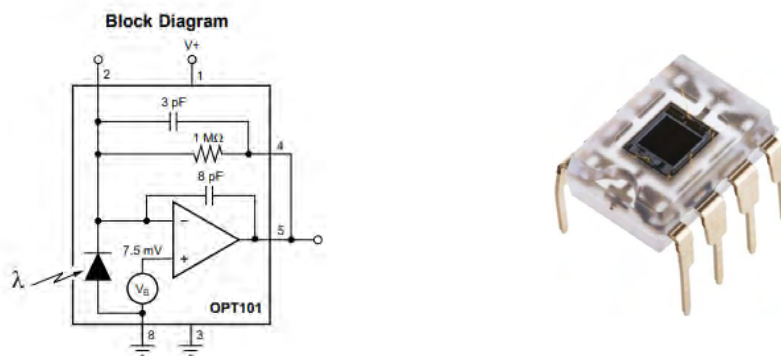


**Figure 39. Block diagram and DIP 8 package of The OPT101.**

The OPT101 is a monolithic photodiode with on-chip trans-impedance amplifier. The integrated combination of photodiode and trans-impedance amplifier on a single chip eliminates the problems commonly encountered in discrete designs, such as leakage current errors, noise pick-up, and gain peaking as a result of stray capacitance. Output voltage increases linearly with light intensity. The amplifier is designed for single or dual power-supply operation and it is housing in a DIP8 package as illustrated in figure 39.

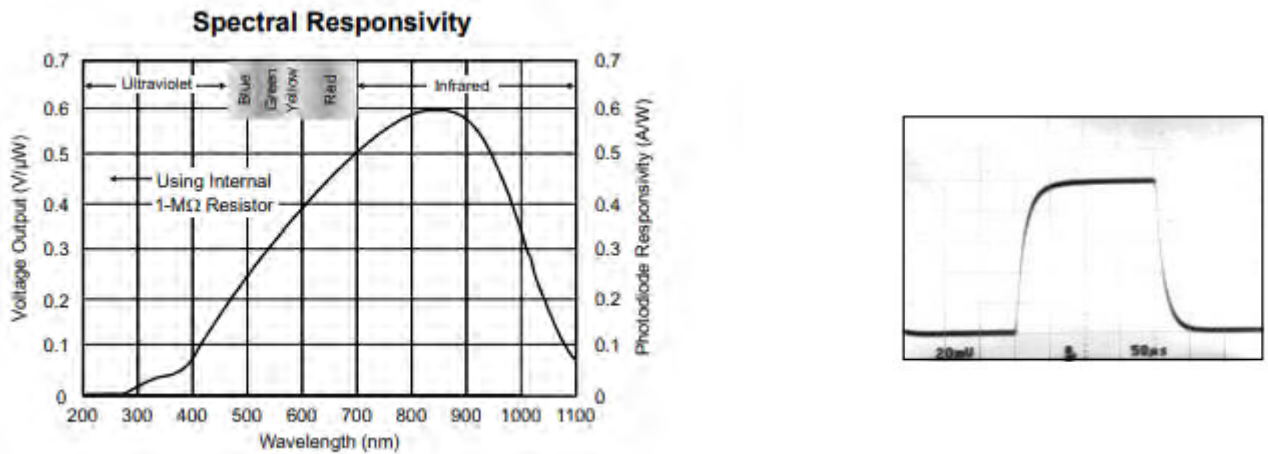


**Figure 40. Spectral Responsivity and Small signal response of OPT101.**

Although the integrated combination of photodiode and trans-impedance amplifier on a single chip is a great feature that OPT101 provides, in practice the receiver was extremely sensitive to disturbances due to ambient light.

As shown in figure 42, the receiving data are placed on top of a 100Hz sinuous disturbance, caused by the fluorescent lights flickering.

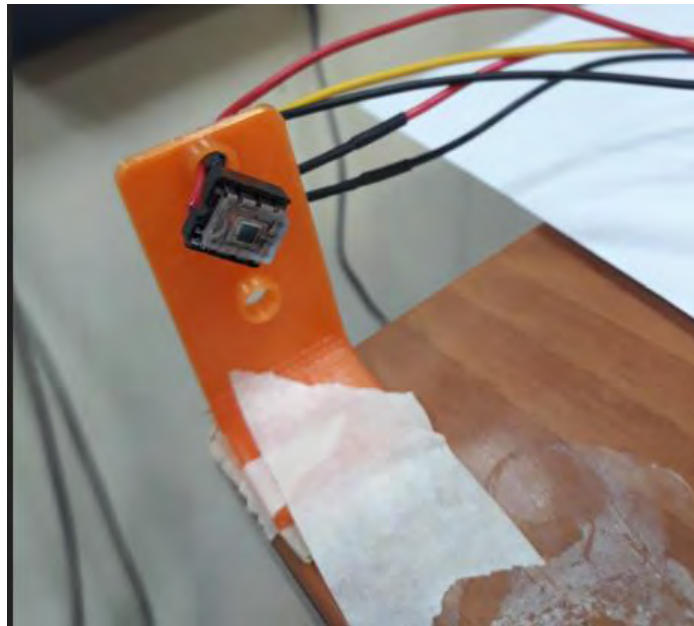


**Figure 41. OPT101 as a receiver**

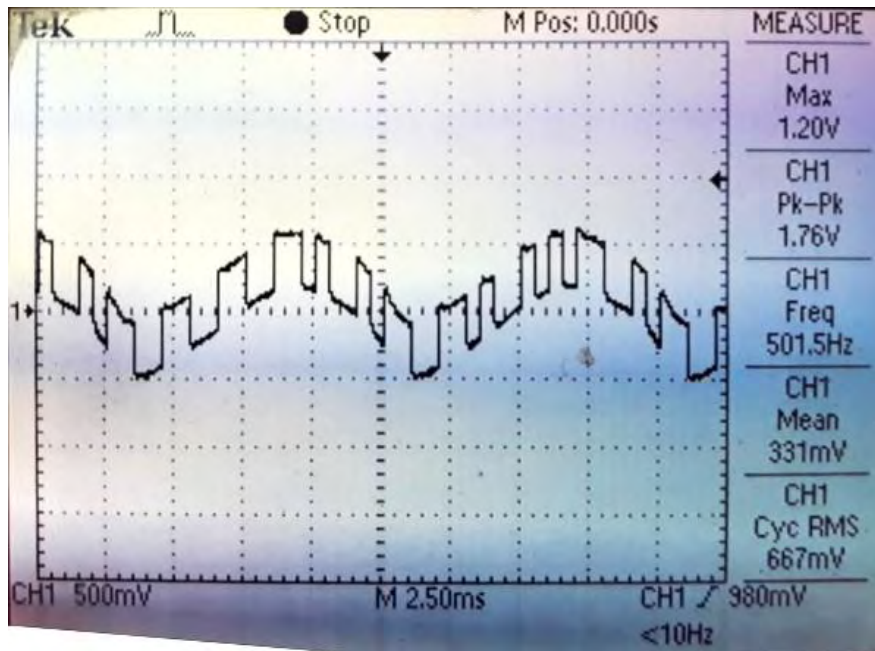


**Figure 42. Fluorescent lights disturbance.**

This effect was present only when the fluorescent lights were on, and it is due to fluorescent lights flickering.

In addition, the receiver was extremely sensitive to any other light sources illuminating around the photodiode, adding random noise or a DC offset to the output, which was hard to remove. OPT101's wide spectral response enables reception from 400nm to 1000nm as shown in figure 41. This wide spectral responsivity, theoretically may increase the bandwidth of a VLC system, but in the current implementation that the bit rate is very low, it only increases the disturbances.

As a result, even though the receiver was working well when lights were Off, this solution found to be problematic, because of the serious interference from other light sources.

#### 7.1.2.2 TLCR5800 LED as a receiver v.1

The second approach included the usage of a LED as a receiver, with a  $1M\Omega$  resistor connected in parallel (figure 43).

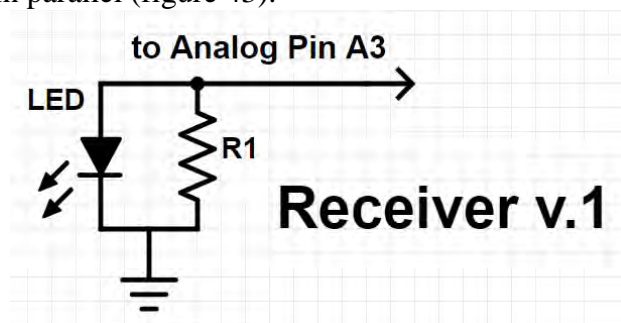


**Figure 43. LED as a Receiver v.1**

Many different types of LEDs were investigated: Blue clear, Green, Red ultra – bright, RGB, and pc-white. The same type of LED was used as emitter and receiver. Red

clear bright LED found to have the best performance and finally the TLCR5800, RED Ultra- bright LED by Vishay was selected.

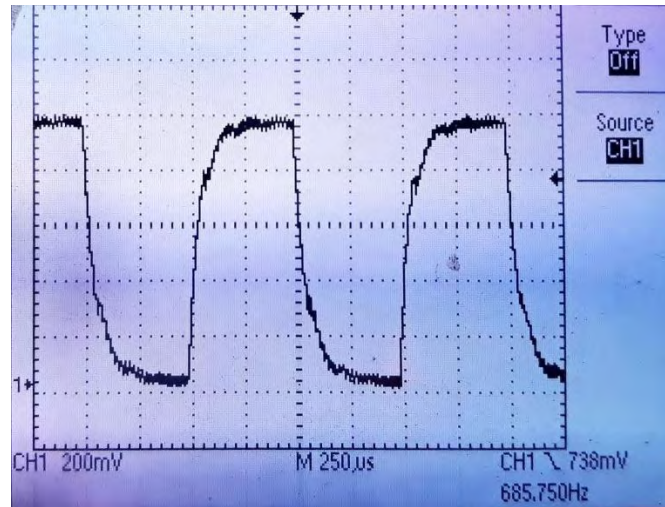


**Figure 44. Data as received from TLCR5800 LED (distance: 10cm) S/N = 26db**

Data as received from the TLCR5800 LED receiver from a very close distance (~10cm) illustrated in figure 44.

Data seem to be clear enough, with a 1V amplitude and the noise level is low (50mV). Pulse shape is as it was expected. Rising  $t_r$  and falling time  $t_f$  are:  $t_r = 120\mu\text{sec}$  and  $t_f = 200\mu\text{sec}$  respectively.

As the distance increases, the noise becomes dominant and shape of receiving data becomes fuzzy, as shown above in figure 45.

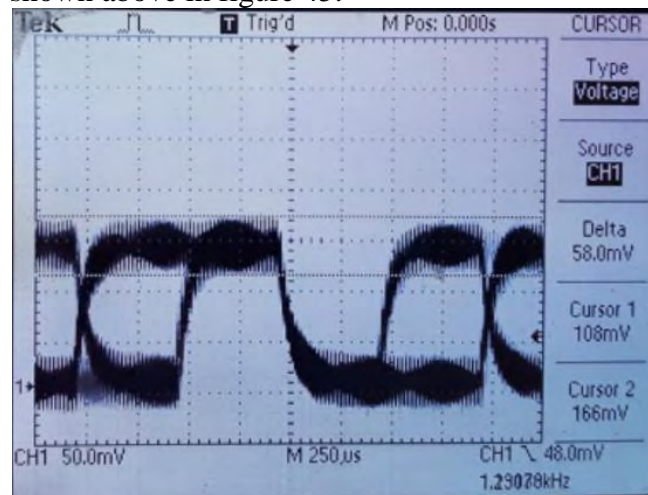


**Figure 45. Data as received from TLCR5800 LED (distance: 30cm) S/N = 9.5db**

At the distance of 30cm, received data now have a significant lower amplitude of 150mV and the noise level remains constant at 50mV. No affect at the Rising  $t_r$  and falling time  $t_f$ . Signal to Noise ratio is now S/N = 9.5db. The usage of an amplification circuitry is now obvious in order to increase the range.

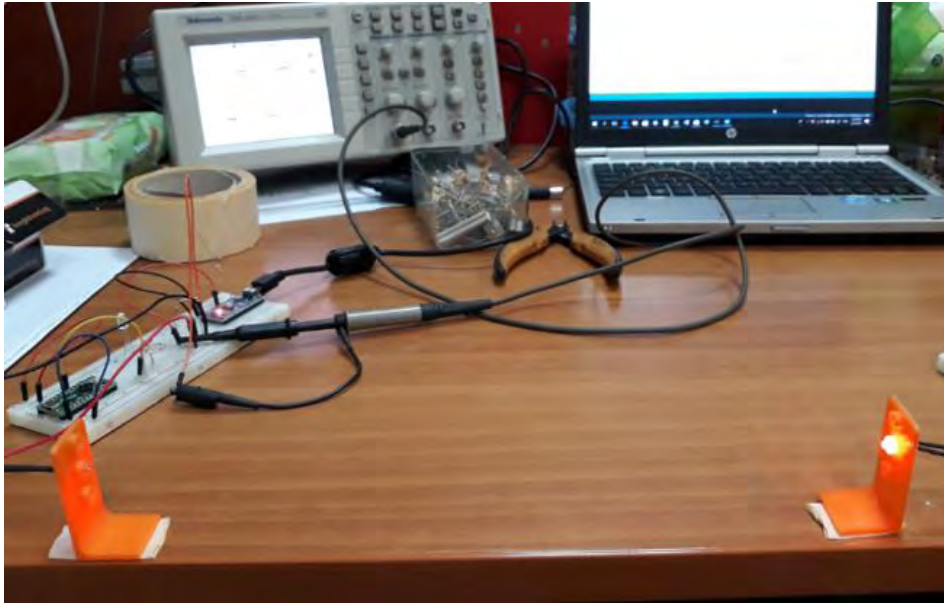


**Figure 46. The experimental setup**

The so far experimental setup is shown in figure 46. The illuminating LED on the right is the emitter and the one on the left is the receiver.

### 7.1.2.3 TLCR5800 LED as a receiver v.2

The designed VLC receiver contains three parts:

- a. a trans-impedance amplifier (TIA) for converting optical signals to electrical voltage,
- b. the proposed Offset Remover stage (OR) for tracking and removing the DC Offset of the converted voltage signal
- c. and a Voltage Comparator (VC) for the final signal conditioning.

Figure 47 illustrates the block diagram, Figure 48 the schematic diagram and Table 5 the component list for the designed and implemented VLC Receiver.

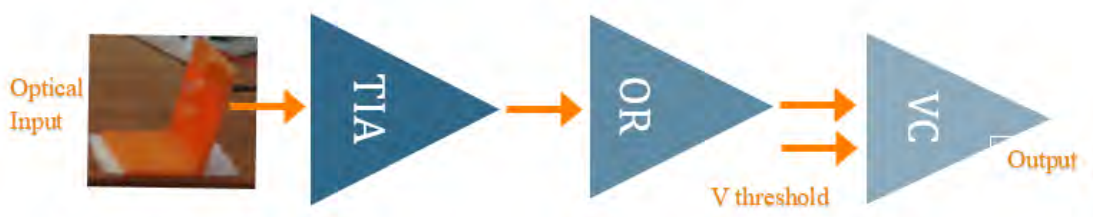


**Figure 47. System block diagram of the implemented VLC receiver v.2**

Part	U1A	U2A/B	Q1	R1	R2pot	R3pot	R4pot	C1	C9
Value	TLC272	LM358	BC557	330K	10K	10K	10K	13pF	1uF

**Table 5. Component list for the designed VLC receiver.**

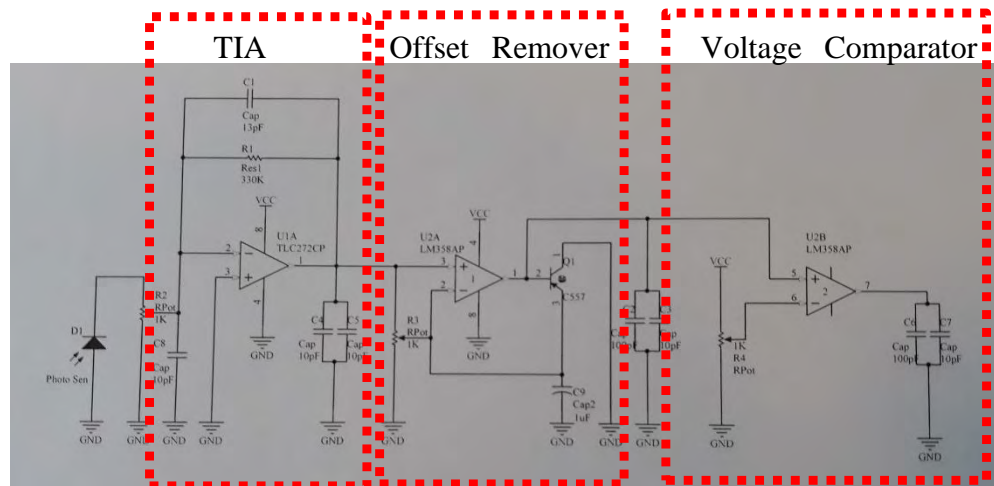


**Figure 48. LED as a Receiver v.2 – The VLC receiver amplification circuit.**

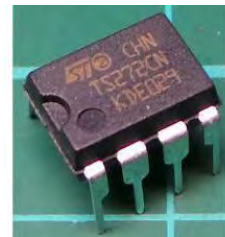
- Trans-impedance amplifier (TIA)

The TLC272 Operational Amplifier by Texas instruments was selected for the TIA stage. The TLC272 precision dual operational amplifier combine a wide range of input offset voltage grades with low offset voltage drift, high input impedance, low noise, and speeds approaching those of general-purpose BiFET devices.

TLC272 OpAmp uses Texas Instruments silicon-gate LinCMOS™ technology, which provides offset voltage stability far exceeding the stability available with conventional metal-gate processes. The extremely high input impedance, low bias current, and high slew rate make TLC272 Op-Amp ideal for VLC applications.

The TLC272 main features include:

- Single-Supply Operation
- Low Noise ...Typically 25 nV/√Hz at f = 1 kHz
- High Input impedance . . . 10<sup>12</sup> Ω Typ
- Input bias current below 5 pA
- Slew rate at Unity-gain bandwidth 2MHz
- unity gain 2.9 V/μs
- Unity-gain bandwidth 2MHz



The frequency response of the TIA stage, as simulated with TINA-TI software, is shown in Figure 49.

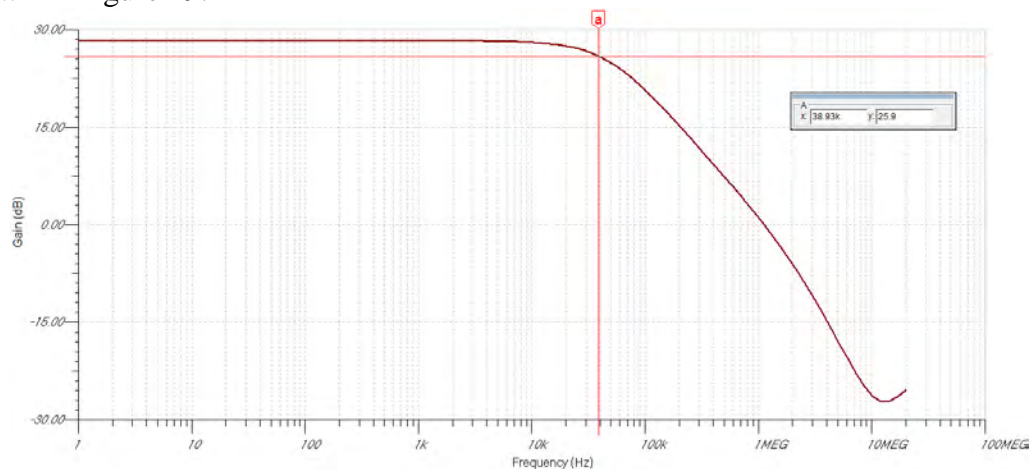


**Figure 49. TIA's stage Frequency response.**

- The Offset Remover stage (OR)

The Offset Remover (OR) stage, includes an LM358 Op-Amp (U2A), a BC557 BJ Transistor (Q1), a 1 $\mu$ F capacitor (C9) and a 10K potentiometer (R3).

As previously mentioned, the on-off keying (OOK) modulation scheme is simple to implement, however it often suffers from the interference caused by ambient lights. At the receiver, received optical signals typically contain the modulated OOK signal, a direct current (DC) component from the sunlight, and a rectified sine wave emitted from indoor fluorescent lights (its frequency is double of the power grid's). The DC component from the sunlight and the rectified sine wave cannot be removed by using capacitors or applying high-pass filtering, as the OOK signal itself also contains a significant DC component.

Essentially, the interference from ambient lights is of additive nature to the modulated information, and all the received optical signals are superimposed together. Hence once the interference level is known at the receiver, the modulated signal can be directly recovered. For the case of OOK modulation, as zero and a high voltage are used to represent digital '0' and '1', the minimum voltage of the OOK signal directly represents the additive interference. Based on this concept, an adaptive minimum – voltage detection circuit is used to remove the interference from ambient lights for OOK modulation.

Due to the above mentioned constrains, the Offset Remover stage (OR) designed in order to charge C9 capacitor when the minimum amplitude of the signal increases. Ideally, charging of C9 is only required during the low-amplitude bit period of the OOK signal, and also when the low amplitude increases with time. However, as it is impossible to predict when the low amplitude of a random OOK signal arrives at the input, a voltage divider is used, meaning that the capacitor is being constantly charged through R3.

The charging/discharging rate of C depends on both the emitter current Q1, and the capacitance of C9. When the voltage at the '+' terminal is lower than that at the '-' terminal, to ensure that C9 can be discharged promptly.

When the voltage at the '+' terminal is higher than that at the '-' terminal, the emitter current of Q1 cannot be either too low for the voltage across C to reach a new (higher) minimum amplitude during one bit period of the OOK signal, or too high so that the voltage rises too much above the minimum amplitude. From the above discussion, for our adaptive design to be able to track the minimum voltage, it is necessary to find an appropriate capacitance of C according to the bit rate of the input OOK signal.

In the current work, the designed VLC receiver for 10 kbit/s OOK signals is simulated using TINA-TI software and fabricated on a single-sided printed circuit board (PCB), as shown in Fig. 51 . The op amps are selected for their wide bandwidth and high slew rate, in order to process high data rate OOK signals.

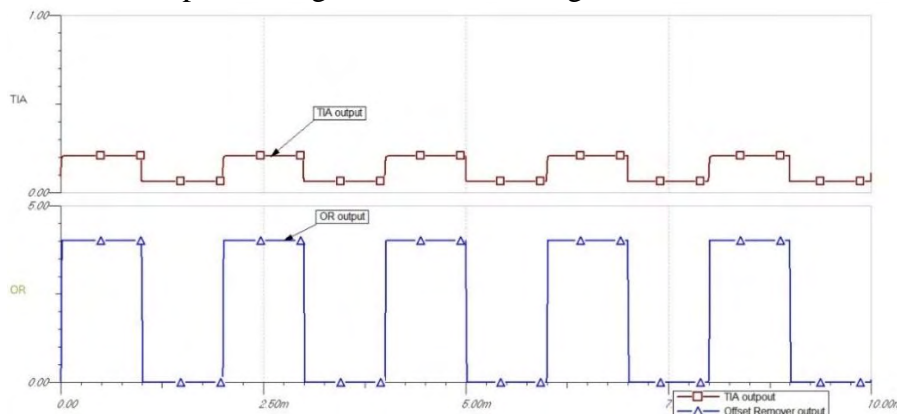


**Figure 50. TIA and OR stages Simulation outputs.**



The above figure 50, illustrates the simulated TIA and OR stages Simulation outputs by TINA-IT software. It is clear that the Offset Remover stage, successfully removes a 100mV DC offset voltage which is present at the TIA output stage.

- The Voltage Comparator (VC)

Finally, a Voltage Comparator (VC) is used for the final signal conditioning. A V reference DC voltage is used as a voltage threshold, representing the average noise level in the circuit, and the VC produces at the output a clear, well-shaped, sharp pulse stream.

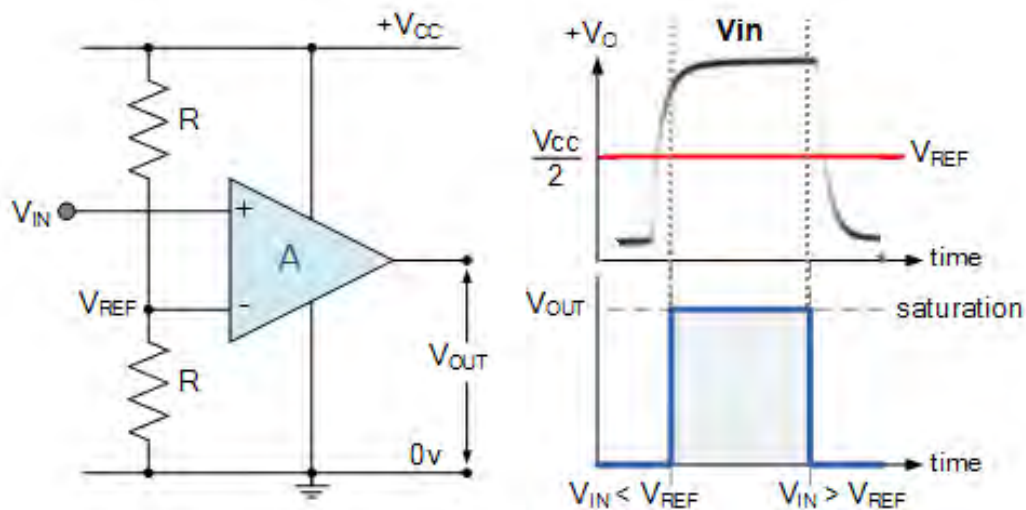


**Figure 51. The Voltage Comparator stage**

This stage also eliminates the effect of wide rising  $t_r$  and falling time  $t_f$  of the transmitted pulse, due to the existence of LED's junction capacitance  $C_j$ . This phenomenon causes various problems, especially at high bit-rates where the sampling rate is high.

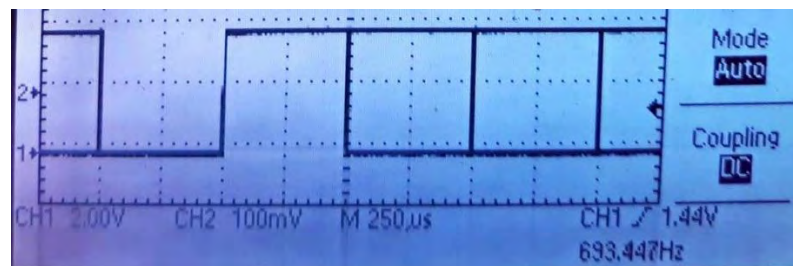


**Figure 52. Data at the Receiver's-v.2 output.**

The final signal as comes out of the receiver v2 is shown in figure 52. Its shape is a perfect pulse stream, noise is not present, DC offset has been removed,  $t_r$  and  $t_f$  times are tend to zero and nor other ambient disturbances exists.

#### 7.1.2.4 Receiver v.2 shield

A receiver PCB board was designed and fabricated in order to minimize any EM noise disturbances and to achieve better mechanical durability. Schematics, simulation and PCB drawings ware designed with a CAD Design Software, and the prototype board milling / drilling procedure was manufactured with a personal CNC machine. Fabrication

stages of the receiver “shield” are shown in figure 53 and the final receiver board, connected on top of the Arduino nano board is shown in figure 54.

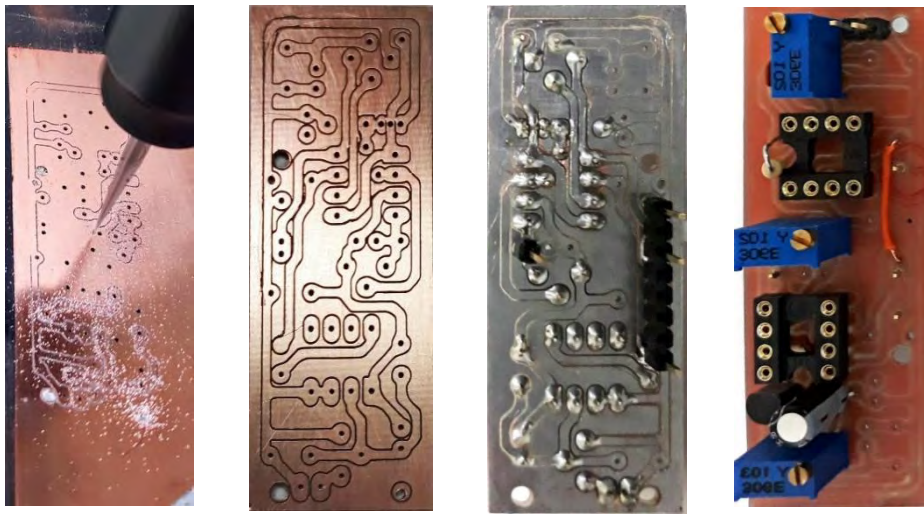


**Figure 53. Receiver v.2 PCB – fabrication stages.**

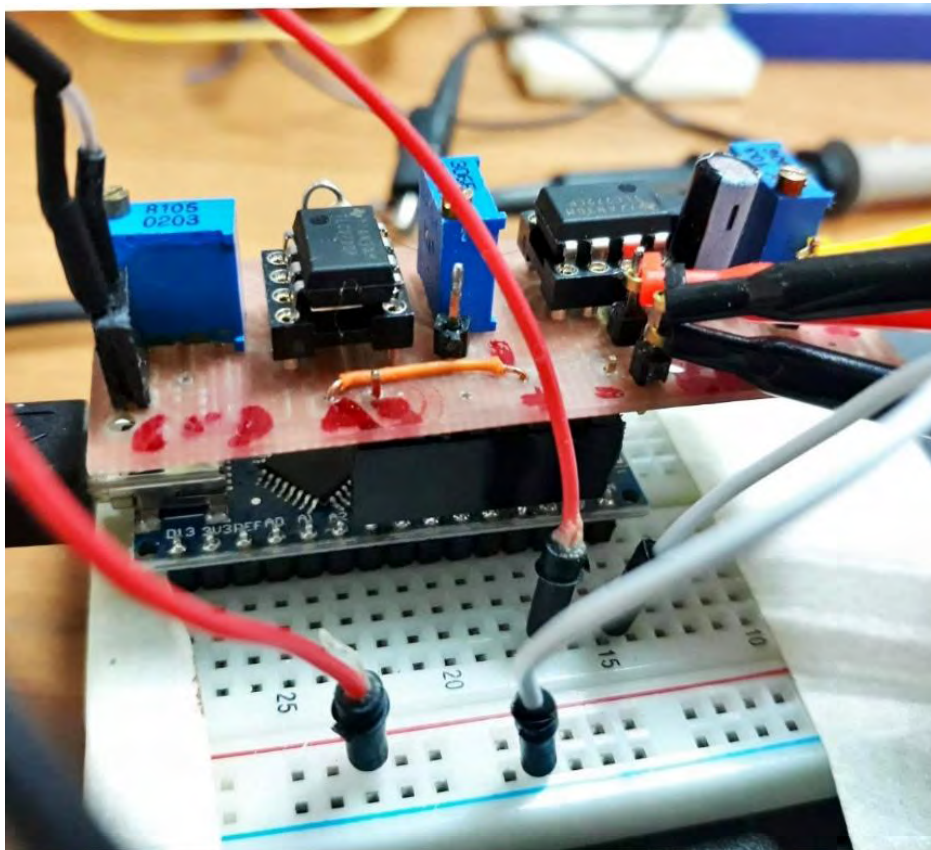


**Figure 54. Receiver v.2 shield**

## 7.2 Software

The code is written in C language, and both microcontrollers used as transmitter and receiver was programmed with the Arduino IDE software.

Both Arduino nano and teensy LC board also programed as a transmitter units and an Arduino nano as a receiver.

In some parts of the code, “bit math” was used instead of DigitalRead(), DigitalWrite() and AnalogRead() Arduino functions, for faster bit manipulation.

A more detailed description about the code is following bellow.

### 7.2.1 Frame format

To help with the synchronization of the receiver and emitter, the data to send (Message) is encapsulated into a frame. This frame is composed of a synchronization preamble (0xAA) that helps to compute the “binarization” threshold. A 0xD5 SYNC Byte then breaks the synchronization (helps detecting the manchester encoding phase), and a STX (0x02) symbol indicate the start of the Data message. A sequence of maximum 32 bytes then follows and a ETX (0x03) ends the transmission. The frame format is shown in table 6.

Data Frame - max length: 38 chars					
[0], [1], [2]	[3]	[4]	[5+ Data size -1]	[37]	
<b>Preamble</b>	<b>SYNC</b>	<b>STX</b>	<b>DATA</b>	<b>ETX</b>	
AA	D5	02		03	(HEX)
01010101	11010101	00000010	D A T A	00000011	(Binary)
3	1	1	(Max 32)	1	Length (Bytes)

**Table 6. Frame Format**

This simple frame structure helps with synchronization recovery but a better frame model would be to add a CRC for error detection in the frame.

### 7.2.2 Emitter’s code

Briefly, the emitter’s code initializes digital port D2 as a digital output, creates the Data Frame to be transmitted [32Bytes], setups the Timer 1 as an interrupt resource every Symbol\_Period time (500usec), reads the Data Frame, encodes it in Manchester code, and transmits serially the Data.

As mentioned above, in a real VLC system, it’s not possible to just serialize the data to transfer and use each serial bit to drive a light source. Doing so would result in a variation of the light source that can be seen with the naked eye and even with fast transmitting speed (and perceived light intensity would depend on the data).

A simple way to encode the data bits that does not affect the perceived lighting is Manchester encoding of the bits. In Manchester encoding a bit is not represented as a steady state of the signal but as a variation (figure 55).

For example a bit with value one will be encoded by the signal going from the low state to the high state and a zero will be encoded by the signal going from the high state to the low state. For a light source this mean that the light quantity averaged over a period of time will no vary over time (for a light source blinking faster than 25Hz, the eye acts as a low-pass filter that average the light quantity).

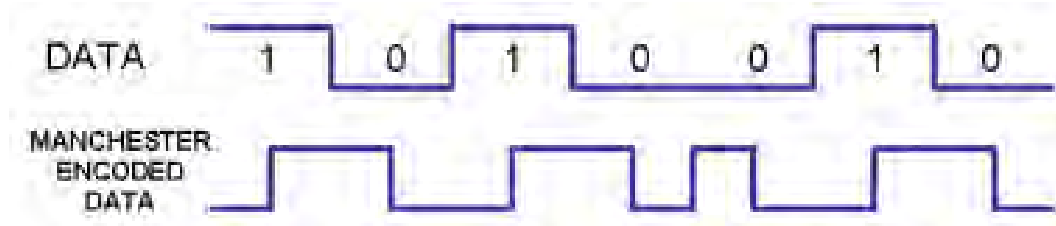


**Figure 55. Manchester Encoding**

So data to send is a just serialized (with a start and a stop bit) and Manchester encoded to drive the LED. As a consequence the LED appears to be ON all the time for the user. The data is sent with a symbol rate of 1000baud which correspond to a bit rate of 500 bit/s. Depending on the led quality and ambient light, the baud rate could be increased.

A flow diagram of the emitter's code is illustrated in figure 56.

### 7.2.3 Receiver's code

The receiver code, uses Analog Input 0 to read the received data. The voltage of the receiver shield is captured by the ADC four time faster than the emitter rate. The voltage is averaged over time to compute a threshold to discriminate high and low state of the incoming signal. This threshold is used to "binarize" the signal and then decode the Manchester encoding. The serial signal is then decoded (detection of start and stop bit) into a byte stream and the data message.

Receiver can be in one of the following state depending of the receiving process.

- 1) IDLE
- 2) SYNC
- 3) START
- 4) DATA

In the IDLE status, receiver has not been synchronized yet and is waiting for a Synchronization byte 0xD5. When the Synchronization byte has been received and decoded, receiver is on SYNC mode, ready to receive the Start of Transmission byte. Since the STX byte has received, receiver goes to START state where it is ready for Data reception. Finally, in DATA state, receiver is receiving Data. A flow diagram of the receiver's code is illustrated in figure 57.

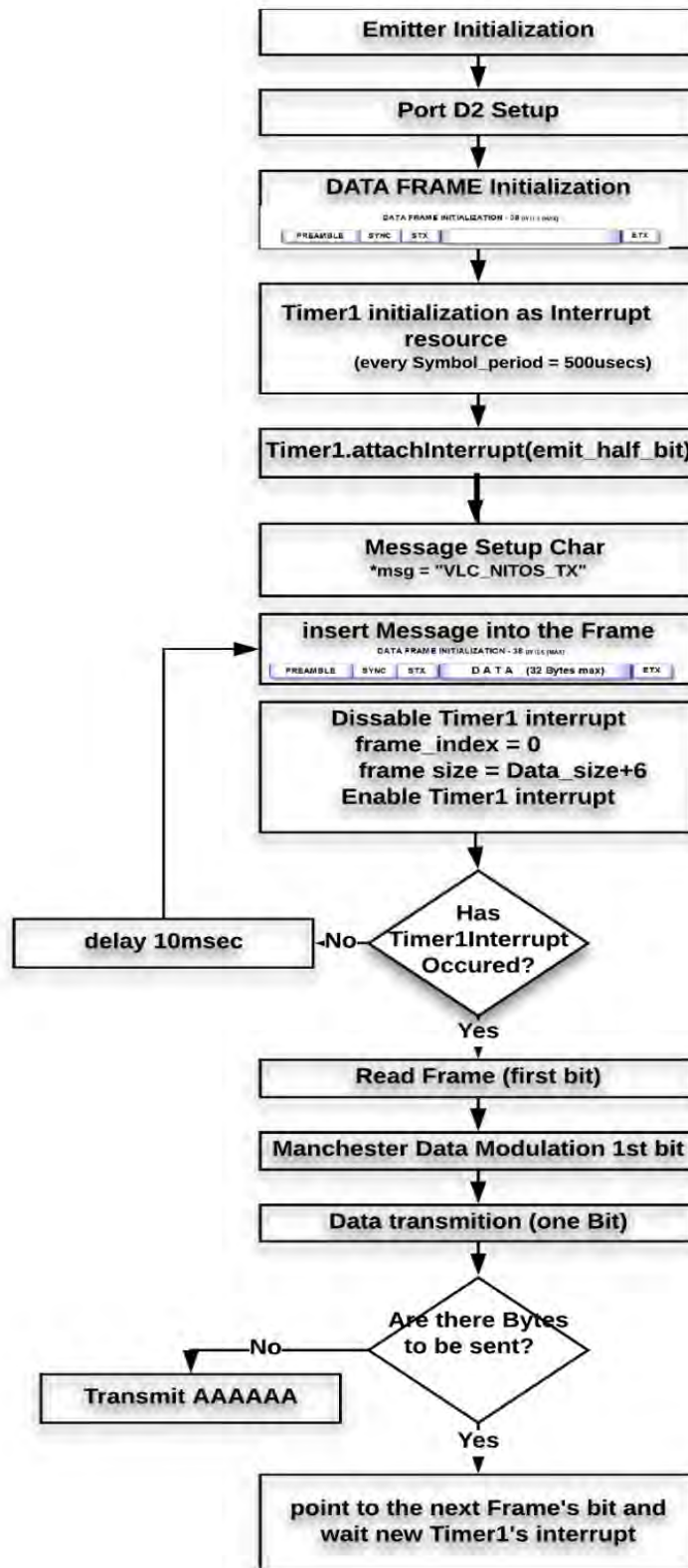


Figure 56. A flow diagram of the emitter's code

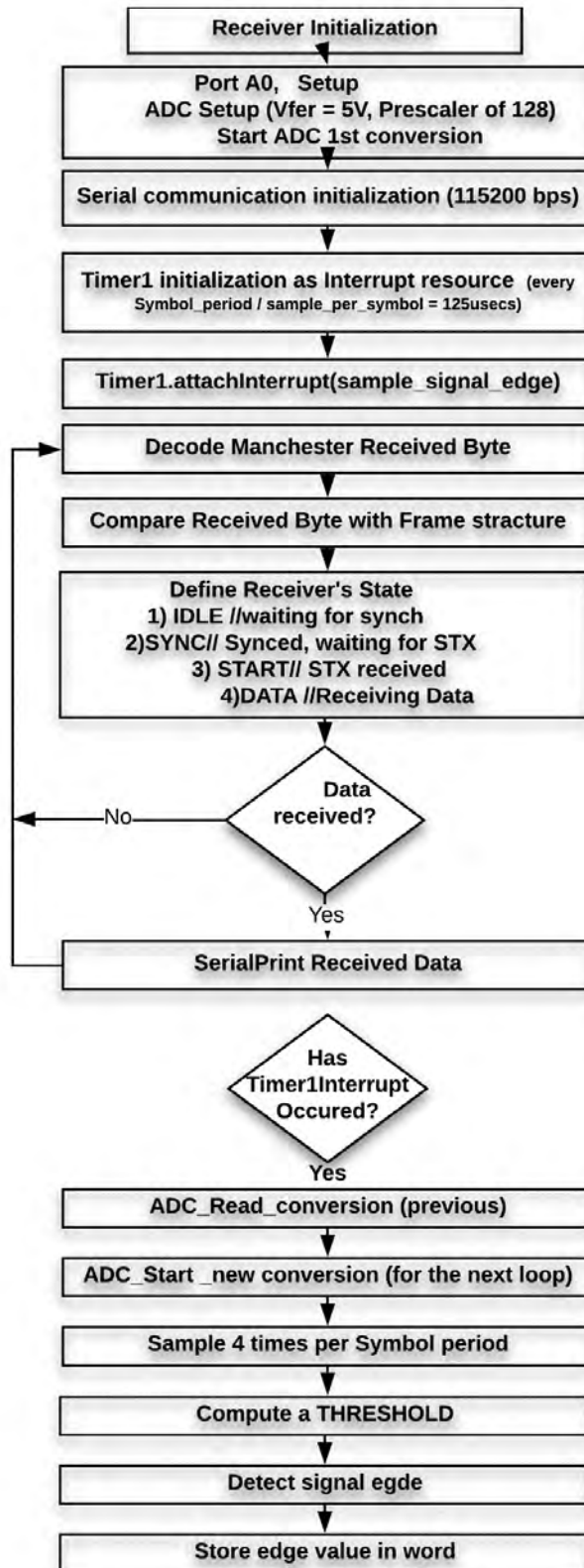


Figure 57.A flow diagram of the receiver's code

### 7.3 Results

The first interesting result that came up during this master thesis research, is that the usage of a LED as light receiver in a real VLC system is feasible. In this case the LED generates a small current which is converted into voltage by the TIA.

Many different types of LEDs was investigated: Blue clear, Green, Red ultra – bright, RGB, and pc-white. The same type of LED was used as emitter and receiver. TLCR5800 Red clear ultra-bright LED found to have the best performance, as shown in table 7 and in following charts in figure58.

LED type	Max Distance (cm)
Green clear	8cm
Blue clear	10cm
Pc white	22cm
Red clear	30cm
TLCR5800 – Red clear ultra-bright	220cm

**Table 7. Different LEDs -Distance Performances using both the final Driver and Receiver circuits**

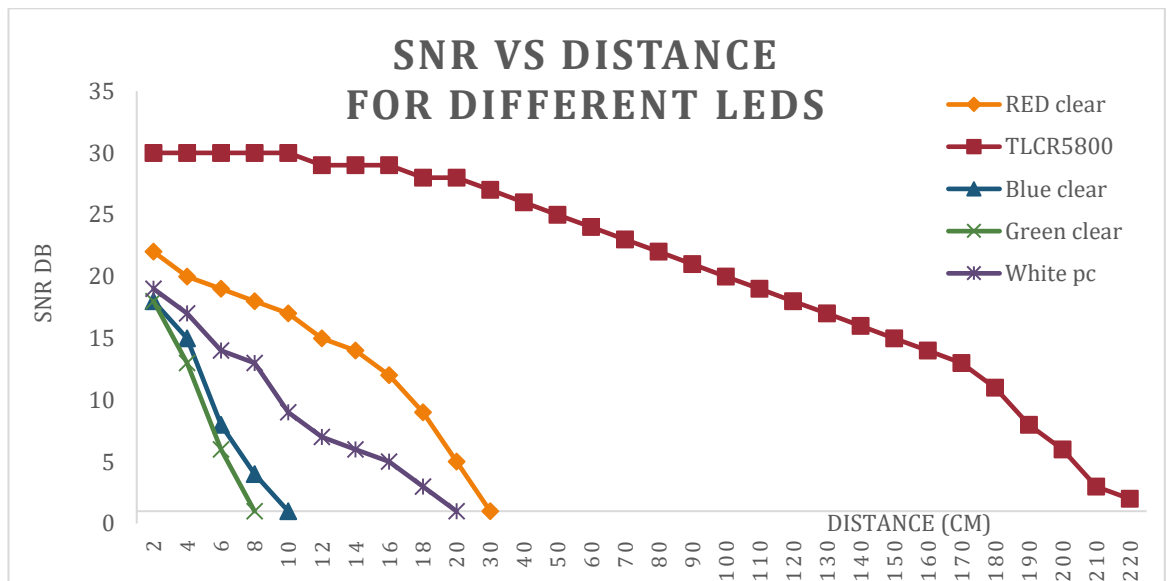





**Figure 58. LED's SNR vs Distance**

After many experimentations and research, TLCR5800, a RED Ultra- bright LED by Vishay was selected for both emitting and receiving LED component.

None of the LEDs tested as receivers was sensitive to flickering caused by fluorescent lights, nor to ambient light / sunlight (Table 8).

The Ambient light causes an unwanted DC offset in the received bit stream, but it is successfully removed in the Offset Remover stage (OR) of the receiver v2 as described above.

	Fluorescent Lights ON 	Sunlight present 	Dark 
LED type	Max Distance (cm)	Max Distance (cm)	Max Distance (cm)
Green clear	8cm	8cm	8cm
Blue clear	10cm	10cm	10cm
Pc white	22cm	22cm	22cm
Red clear	30cm	30cm	30cm
TLCR5800 - Red clear ultra-bright	220cm	220cm	220cm

**Table 8. Distances under different ambient lighting conditions**

Another interesting note is that ideally a LED works as a selective sensor, meaning that for instance a blue LED will capture (mainly) blue light (same for red and green). A white LED won't work exactly in the same way, since a white-pc LED is just a blue LED with phosphor coating.

In practice though, as discussed in chapter 4.2 “LED as a photodiode”, the responsivity curve of a LED is shifted towards lower wavelengths (or higher energy photons) with reference to the peak of LED emission spectra.

This phenomenon was examined and confirmed, since the TLCR5800 which is a RED Ultra- bright LED, was able to successfully detect light pulses that were emitted by Green, Blue and White LEDs. Communication distance in that case was reduced.

Apart from the LED, the rest of the hardware (transmitter / receiver) was also tested.

Transmitter’s circuit, far simpler compared to the receiver, was examined in both the time and frequency domain, where the expected behaviour was confirmed up to 100kbps, without any serious distortions. The usage of a Baker clamp driver was not considered necessary, since the bit-rate was just 1kbps.

Receiver’s circuit, tested and examined too, giving the expected results up to 15kbps. The operation of the receiver – shield is characterized as sufficient, since it is capable of receiving low intensity signals, distinguishing the signal from noise, removing any DC offset caused by ambient lighting, and forming a pulse stream which can safely be sampled by the microcontroller’s ADC

The “eye pattern” in figure 59, illustrates the quality of the pulse stream at the output of the receiver-v.2 shield at 1kbps / 100cm distance.

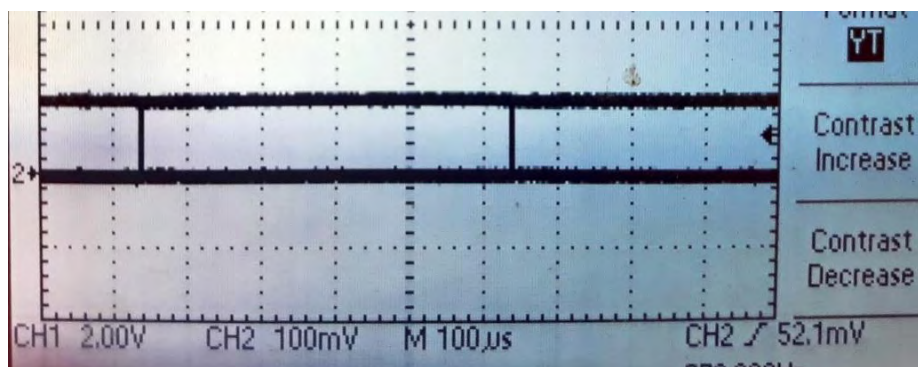


**Figure 59. "Eye pattern" at 1kbps.**



Receiver's response found to be the same up to 15 KHz, due to high gain and the 2MHz unity-gain bandwidth of the TLC272 Op-Amp.

In practice, the receiver shield is behaving as expected only up to approximately 15 kHz. This limitation does not affect the current implementation, since the bit rate is much lower (1kbps).

Special effort took place, in order to increase the communication range. A second TLCR5800 LED emitter was then added just next to the first one, as shown in figure 59.

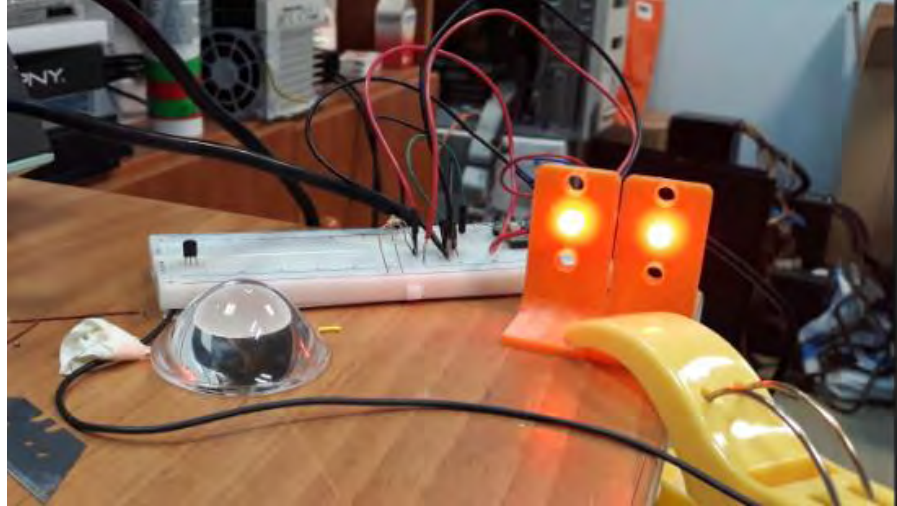


**Figure 60. A Second LED emitter “in parallel”**

The optical power of the signal was increased and so the distance and BER was also increased and the optical link was more immune in terms of emitter - receiver alignment.

In conclusion, the VLC system was examined and worked in a sufficient behaviour for its initial specifications. It is obvious that the current implementation is just an extremely basic approach to a very promising technology which is rapidly developing!

# 8 REFERENCES

- [1] Shlomi Arnon, John Barry, George Karagiannidis, Robert Schober, and Murat Uysal, eds. *Advanced “Optical Wireless Communication Systems”*. Cambridge University Press, 2012.
- [2] IEEE 802.15.7 “Visible Light Communication: Modulation Schemes and Dimming Support”
- [3] figure1: Navin Kumar, “Visible Light Communication in Intelligent Transportation Systems”, IEEE International Conference of communication, 2014.
- [4] D. Malacara, *Color Vision and Colorimetry: Theory and Applications*, 2nd edition, SPIE, Bellingham, WA, 2011.
- [5] G. Wyszecki and W. S. Stiles, *Color Science: Concepts and Methods, Quantitative Data and Formulae*, Wiley Classics Library Edition, 2nd Edition, Hoboken, NJ, 2000.
- [6] S. M. Sze, *Physics of Semiconductor Devices*, 3rd edition, Wiley, Hoboken, NJ, 2008.
- [7] E. F. Schubert, *Light-Emitting Diodes*, 2nd edition, Cambridge University Press, Cambridge, UK, 2006.
- [8] S. Rajbhandari, H. Chun, G. Faulkner, K. Cameron, A. V. N. Jalajakumari, R. Henderson, D. Tsonev, et al., *High-Speed Integrated Visible Light Communication System: Device Constraints and Design Considerations*, IEEE J. Sel. Areas Commun., vol. 33, no. 9, pp. 1750–1757, 2015.
- [9] N. Mohan, T. M. Undeland and W. P. Robbins, *Power Electronics: Converters, Applications and Design*, 3rd edition, Wiley, Hoboken, NJ, 2003.
- [10] J. Millman and C. Halkias, *Integrated Electronics*, 2nd edition, MacGraw Hill, New York, NY, 1972.
- [11] P. Gray and R. Meyer, *Analysis and Design of Analog Integrated Circuits*, Wiley, Hoboken, NJ, 1984.
- [12] M. Wolf, J. Vucic, D. O’Brien, O. Bouchet, H. Le Minh, G. Faulkner, L. Grobe, et al., *Deliverable 4.2a—Physical Layer Design and Specification: Demonstrator 1*, FP7/ICT 213311, European Commission, Brussels, Belgium, 2010.
- [13] O. Bouchet, G. Faulkner, L. Grobe, E. Gueutier, K.-D. Langer, S. Nerreter, D. O’Brien, et al., *Deliverable 4.2b—Physical Layer Design and Specification: Demonstrator 2*, FP7/ICT 213311, European Commission, Brussels, Belgium, 2011.
- [14] C. Toumazou, F. J. Lidgley and D. G. Haigh, *Analogue IC Design: The Current-Mode Approach*, IEE Circuits, Devices and Systems Series, Peter Peregrinus Ltd, USA, 1990.
- [15] H. Li, Y. Zhang, X. Chen, C. Wu, J. Guo, Z. Gao, W. Pei and H. Chen, *682Mbit/s Phosphorescent White LED Visible Light Communications Utilizing Analogue Equalized 16QAM-OFDM Modulation without Blue Filter*, Elsevier, J. Opt. Commun., vol. 354, pp. 107–111, 2015.
- [16] X. Huang, Z. Wang, J. Shi, Y. Wang and N. Chi, *1.6 Gbit/s Phosphorescent White LED Based VLC Transmission using a Cascaded Pre-equalization Circuit and a Differential Outputs PIN Receiver*, OSA Opt. Express, vol. 23, no. 17, pp. 22034–22042, 2015.
- [17] R. L. Aguiar, A. Tavares, J. L. Cura, E. de Vasconcelos, L. N. Alves, R. Valadas and D. M. Santos, *Considerations on the Design of Transceivers for Wireless Optical LANs*, IEE Electronics & Communications, Colloquium on Optical Wireless Communications, London, UK, June 1999.
- [18] L. N. Alves, *High Gain and Bandwidth Current-Mode Amplifiers: Study and Implementation*, PhD thesis, Universidade de Aveiro, Aveiro, Portugal, 2008.
- [19] L. N. Alves and R. L. Aguiar, *Design Techniques for High Performance Optical Wireless Front-Ends*, Proceedings of the Conference on Telecommunications—ConfTele 2003, Aveiro, Portugal, April 2003.
- [20] J. J. Morikuni and S.-M. Kang, *An Analysis of Inductive Peaking in Photoreceiver Design*, IEEE J. Lightwave Technol., vol. 10, no. 10, pp. 1426–1437, 1992.
- [21] D. Karunatilaka, F. Zafar, V. Kalavally, “LED Based Indoor Visible Light Communications: State of the Art”, IEEE COMMUNICATION SURVEYS & TUTORIALS, VOL. 17, NO. 3, THIRD QUARTER 2015
- [23] *natural resource management to electromagnetic spectrum*, Michigan Telecommun. Technol. Law Rev., vol. 10, no. 2, p. 285, 2004.
- [24] H. Baldwin, “Wireless bandwidth: Are we running out of room?” 2012.
- [25] M. Oh, “A flicker mitigation modulation scheme for visible light communications,” in Proc. 15th ICACT, PyeongChang, Korea, 2013, pp. 933–936.
- [26] B. Love, D. Love, and J. Krogmeier, “Like deck chairs on the titanic: Why spectrum reallocation won’t avert the coming data crunch but technology might keep the wireless industry afloat,” Washington Univ. Law Rev., vol. 89, p. 705, 2012.
- [27] C. Jastrow et al., “300 GHz transmission system,” Electron. Lett., vol. 44, no. 3, pp. 213–214, Jan. 2008.
- [28] I. Hosako et al., “At the dawn of a new era in terahertz technology,” Proc. IEEE, vol. 95, no. 8, pp. 1611–1623, Aug. 2007.
- [29] H. Parikh, J. Chokshi, N. Gala, and T. Biradar, “Wirelessly transmitting a grayscale image using visible light,” in Proc. ICATE, Mumbai, India, 2013, pp. 1–6.
- [30] R. Wood, “Wireless network traffic worldwide: forecasts and analysis 2013–2018,” Analysys Mason Limited, New Delhi, India, Tech. Rep., 2013.
- [31] C. Gabriel, “Wireless broadband alliance industry report 2013: Global trends in Public Wi-Fi,” Marvedis Rethink—Wireless Broadband Alliance, Singapore, Tech. Rep., 2013.
- [32] S. M. Kim and S. M. Kim, “Performance improvement of visible light communications using optical beamforming,” in Proc. 5th ICUFN, Da Nang, Vietnam, 2013, pp. 362–365.
- [33] D. Borah, A. Boucouvalas, C. Davis, S. Hranilovic, and K. Yiannopoulos, “A review of communication-oriented optical wireless systems,” EURASIP J. Wireless Commun. Netw., vol. 2012, no. 1, pp. 91–119, Mar. 2012.
- [34] G. Dede, T. Kamalakis, and D. Varoutas, “Evaluation of optical wireless technologies in home networking: An analytical hierarchy process approach,” IEEE/OSA J. Opt. Commun. Netw., vol. 3, no. 11, pp. 850–859, Nov. 2011. [35] S. Zhao, J. Xu, and O. Trescases, “A dimmable LED driver for Visible Light Communication (VLC) based on llc resonant DC-DC converter operating in burst mode,” in Proc. 28th Annu. IEEE APEC Expo., Long Beach, CA, USA, 2013, pp. 2144–2150.
- [36] M. Biagi, T. Borogovac, and T. Little, “Adaptive receiver for indoor visible light communications,” J. Lightw. Technol., vol. 31, no. 23, pp. 3676–3686, Dec. 2013.
- [37] C. Chow, C. Yeh, Y. Liu, P. Huang, and Y. Liu, “Adaptive scheme for maintaining the performance of the in-home white-LED visible light wireless communications using OFDM,” Opt. Commun., vol. 292, no. 1, pp. 49–52, Apr. 2013.

- [38] Y. Wang, Y. Wang, N. Chi, J. Yu, and H. Shang, "Demonstration of 575-mb/s downlink and 225-mb/s uplink bi-directional SCM-WDM visible light communication using RGB LED and phosphor-based LED," *Opt. Exp.*, vol. 21, no. 1, pp. 1203–1208, Jan. 2013.
- [39] M. J. Eckelman, P. T. Anastas, and J. B. Zimmerman, "Spatial assessment of net mercury emissions from the use of fluorescent bulbs," *Environ. Sci. Technol.*, vol. 42, no. 22, pp. 8564–8570, Nov. 2008.
- [40] S. Bose-O'Reilly, K. M. McCarty, N. Steckling, and B. Lettmeier, "Mercury exposure and children's health," *Curr. Probl. Pediatr. Adolesc. Health Care*, vol. 40, no. 8, pp. 186–215, Sep. 2010.
- [41] T. Katsuura et al., "Effects of blue pulsed light on human physiological functions and subjective evaluation," *J. Physiol. Anthropol.*, vol. 31, no. 1, pp. 1–5, Sep. 2012.
- [42] M. Kavehrad, "Sustainable energy-efficient wireless applications using light," *IEEE Commun. Mag.*, vol. 48, no. 12, pp. 66–73, Dec. 2010.
- [43] K. Pujapanda, "LiFi integrated to power-lines for smart illumination cum communication," in *Proc. Int. Conf. CSNT, Gwalior, India, 2013*, pp. 875–878.
- [44] M. Uddin, M. Chowdhury, and Y. M. Jang, "Priority-based resource allocation scheme for visible light communication," in *Proc. 2nd ICUFN, Jeju Island, Korea, 2010*, pp. 247–250.
- [45] J. Kim and E. Schubert, "Transcending the replacement paradigm of solid-state lighting," *Opt. Exp.*, vol. 16, no. 26, pp. 21835–21842, Dec. 2008.
- [46] N. Bardsley et al., "Solid-state lighting research and development: Multi-year program plan," U.S. Dept. Energy, Washington, DC, USA, Tech. Rep., 2014. [47] A. Jovicic, J. Li, and T. Richardson, "Visible light communication: opportunities, challenges and the path to market," *IEEE Commun. Mag.*, vol. 51, no. 12, pp. 26–32, Dec. 2013.
- [48] D. O'Brien, "Visible light communications: Challenges and potential," in *Proc. IEEE IPC, Arlington, VA, USA, 2011*, pp. 365–366.
- [49] "Infrared data association," Walnut Creek, CA, USA, 2012. [Online]. Available: <http://www.irda.org>
- [50] J. Tuenge, "SSL pricing and efficacy trend analysis for utility program planning," U.S. Dept. Energy, Washington, DC, USA, Tech. Rep., 2013.
- [51] C. Medina, M. Zambrano, K. Navarro, "LED BASED VISIBLE LIGHT COMMUNICATION TECHNOLOGY APPLICATIONS AND CHALLENGES – A SURVEY", *International Journal of Advances in Engineering & Technology*, Aug., 2015
- [52] D. Karunatilaka, F. Zafar, V. Kalavally, R. Parthiban, "LED Based Indoor Visible Light Communications: State of the Art," *IEEE Communications Surveys & Tutorials*, Mar. 2015.
- [53] S. Berman et al., "Human Electroretinogram Responses to Video Displays, Fluorescent Lighting and Other High Frequency Sources," *Optometry and Vision Science*, vol. 68, 1991, pp. 645–62.
- [54] Fan, J.; Mohamed, M.G.; Qian, C.; Fan, X.; Zhang, G.; Pecht, M. Color Shift Failure Prediction for Phosphor-Converted White LEDs by Modeling Features of Spectral Power Distribution with a Nonlinear Filter Approach. *Materials* 2017, 10, 819.
- [55] P. Louro, V. Silva, I. Rodrigues M.A. Vieira M. Vieira, "Transmission of Signals Using White LEDs for VLC Applications", 12th International Conference on Nanosciences & Nanotechnologies & 8th International Symposium on Flexible Organic Electronics, 2016.
- [56] Micro LED: Understand the New Display Technology in 3 minutes, [www.ledinside.com](http://www.ledinside.com), online: <https://www.ledinside.com/news/2017/4/micro-led-understand-the-new-display-technology-in-3-minutes>.
- [57] R. Ji, S. Wang, Q. Liu, Wei Lu, "High-Speed Visible Light Communications: Enabling Technologies and State of the Art", *Applied Sciences* 2018, 8(4), p589.
- [58] 20Shi, J.W.; Sheu, J.K.; Chen, C.H.; Lin, G.R.; Lai, W.C. High-speed GaN-based green light-emitting diodes with partially N-doped active layers and current-confined apertures. *IEEE Electron Device Lett.* 2008, 29, 158–160. [Google Scholar] [CrossRef]
- [59] 19Oh, H.S.; Hue Joo, J.; Lee, J.H.; Hyeob Baek, J.; Seo, J.W.; Kwak, J.S. Structural optimization of high-power algaing resonant cavity light-emitting diodes for visible light communications. *Jpn. J. Appl. Phys.* 2008, 47, 6214–6216. [Google Scholar] [CrossRef]
- [60] P. H. Binh, V. D. Trong, Pierre Renucci, and X. Marie "Improving OOK Modulation Rate of Visible LED by Peaking and carrier Sweep-Out effects Using n Schottky Diodes – Capacitance Circuit.", *JOURNAL OF LIGHTWAVE TECHNOLOGY*, VOL. 31, NO. 15, AUGUST 1, 2013
- [61] Zabih Ghassemlooy, Luis Nero Alves, Stanislav Zvánovec, Mohammad-Ali Khalighi "Visible Light Communications Theory and Applications", CRC Press, 2017.
- [62] P. Dietz, W. Yerazunis, and D. Leigh Very "Low-Cost Sensing and Communication Using Bidirectional LEDs" Mitsubishi Electric Research Laboratories, 201 Broadway Cambridge, Massachusetts 02139 USA
- [63] G. Stepniak, M. Kowalczyk, L. Maksymiuk, J. Siuzdak "Transmission Beyond 100 Mbit/s Using LED Both as a Transmitter and Receiver", *IEEE Photonics Technology Letters* ( Volume: 27, Issue: 19, Oct. 1, 1 2015 ) <https://ieeexplore.ieee.org/document/7140753/?arnumber=7140753&tag=1>
- [64] Light emitting diodes as optical detectors .<http://www.academicos.ccadet.unam.mx/martha.rosete/Leds.htm>
- [65] Akshay Bhat, "Stabilize Your Transimpedance Amplifier", APPLICATION NOTE 5129, Maxim Integrated, 2012 <https://www.maximintegrated.com/en/app-notes/index.mvp/id/5129>
- [66] N. Kumar, M. Figueiredo, L. Nero, A. Rui L. Aguiar "VLC Modulation Schemes" Instituto de Telecomunicações Pólo de Aveiro, March 31st, 2011. <https://ria.ua.pt/bitstream/10773/11870/1/VIDAS%20D4.1%20-%20VLC%20Modulation%20Schemes.pdf>
- [67] <http://visiblelightcomm.com/an-ieee-standard-for-visible-light-communications/manchestercoding/>
- [68] A. PRADANA, N. AHMANDI, "VLC PHYSICAL LAYER DESIGN BASED ON PULSE POSITION MODULATION (PPM) FOR STABLE ILLUMINATION" *2015 International Symposium on Intelligent Signal Processing and Communication Systems (ISPACS)*
- [69] A Review of Modulation Schemes for Visible Light Communication
- [70] Chromaticity diagram. Available: [http://commons.wikimedia.org/wiki/File:Cie\\_chromaticity](http://commons.wikimedia.org/wiki/File:Cie_chromaticity) diagram wavelength.png

# APPENDICES

## *STANDARDIZATION EFFORTS*

# STANDARDIZATION EFFORTS

Initial standardization efforts were undertaken in Japan, by Japan Electronics and Information Technology Industries Association (JEITA) in JEITA standards CP-1221, CP-1222. Later on VLCC, together with Infrared Data Association (IrDA) published IrDA like standards for VLC in 2009. IEEE approved a comprehensive 802.15.7 VLC standard in 2011. It is a task group within the 802.15 working group for Wireless Personal Area Networks (WPAN). It is open to all optical wavelengths from 190 nm (UV) to 10  $\mu\text{m}$  (IR). It is open for various applications including outdoor traffic lighting systems, mobile devices, signboards and other display mechanisms as well as indoor lighting. At the moment, the standard utilizes only single carrier modulation schemes (OOK, VPPM) at a maximum achievable rate of 96 Mb/s, deemed by one of three operating modes (PHYI, PHYII, PHYIII). The standard also introduces CSK modulation for multi colored sources.

- PHYI: For high current, low bandwidth outdoor devices such as traffic lights. It uses OOK and VPPM with data rates up to 266 Kb/s.
- PHY II: For indoor use for mobile devices and displays with high bandwidth, low power transmitters as well as lighting systems. It also uses OOK and VPPM with data rates up to 96 Mb/s.
- PHYIII: CSK modulation utilizing multi-chip LEDs can provide data rates up to 96 Mb/s. A source capable of modulating CSK will have to comply to wavelength band plan where the peak emission wavelength lies.

Furthermore, the system utilizes flicker mitigation mechanisms and three types of dimming schemes, Cellular structure with handover mechanism to support user mobility, as well as three multi-access topologies (Point to point, Star, Broadcast).

Recently, some developments in using American National Standards Institute (ANSI) E1.11 entertainment lighting standards to provide low data rate VLC data to luminaries has emerged. This standard is generally referred to as DMX512, and is used mainly in theatre lighting systems control. The application scenarios include guiding viewers to seats in theatres, lighting control troubleshooting, as well as supermarket navigation. The draft mechanism packs IEEE 802 data frames into an ANSI E1.11 link using a proposed E1.45 packet format. Simultaneous lighting control and unidirectional VLC communication would be possible with this methodology.